

Rothamsted Repository Download

A - Papers appearing in refereed journals

Rose, T., Wilkinson, M. D., Lowe, C., Xu, J., Hughes, D. J., Hassall, K. L., Hassani-Pak, K., Amberkar, S., Noletto-Dias, C., Ward, J. L. and Heuer, S. 2022. Novel molecules and target genes for vegetative heat tolerance in wheat. *Plant Environmental Interactions*. 3 (6), pp. 264-289.
<https://doi.org/10.1002/pei3.10096>

The publisher's version can be accessed at:

- <https://doi.org/10.1002/pei3.10096>

The output can be accessed at: <https://repository.rothamsted.ac.uk/item/989w5/novel-molecules-and-target-genes-for-vegetative-heat-tolerance-in-wheat>.

© 26 December 2022, Please contact library@rothamsted.ac.uk for copyright queries.

1 Novel molecules and target genes for vegetative heat tolerance in wheat

2
3 Teresa Rose¹, Mark Wilkinson¹, Claudia Lowe¹, Jiemeng Xu¹, David Hughes¹, Kirsty L. Hassall¹, Keywan
4 Hassani-Pak¹, Sandeep Amberkar^{1,2}, Clarice Noleto-Dias, Jane Ward¹, Sigrid Heuer^{1,3*}

5
6 ¹Rothamsted Research, Harpenden, UK

7 ²Institute of Systems, Molecular and Integrative Biology, University of Liverpool, UK

8 ³National Institute of Agricultural Botany (NIAB), Cambridge, UK

9
10 *Corresponding author

11 **Abstract**

12
13 To prevent yield losses caused by climate change it is important to identify naturally tolerant
14 genotypes with traits and related pathways that can be targeted for crop improvement. Here we
15 report on the characterization of contrasting vegetative heat tolerance in two UK bread wheat
16 varieties. Under chronic heat stress, the heat-tolerant cultivar Cadenza produced an excessive number
17 of tillers which translated into more spikes and higher grain yield compared to heat-sensitive Paragon.
18 RNAseq and metabolomics analyses revealed a set of about 400 heat-responsive genes common to
19 both genotypes. Only 71 genes showed a genotype x temperature interaction. As well as known heat-
20 responsive genes such as HSPs, several genes that have not been previously linked to the heat
21 response, particularly in wheat, have been identified, including several dehydrins, a number of
22 ankyrin-repeat protein-encoding genes, and lipases. Over 5000 genotype-specific genes were
23 identified, including photosynthesis-related genes which might explain the observed ability of
24 Cadenza to maintain photosynthetic rate under heat stress. Contrary to primary metabolites,
25 secondary metabolites showed a highly differentiated heat response and genotypic differences. These
26 included e.g., benzoxazinoid (DIBOA, DIMBOA) but in particular phenylpropanoids and flavonoids with
27 known radical scavenging capacity, which was assessed via the DPPH assay. The most highly heat-
28 induced metabolite was (glycosylated) propanediol, which is widely used in industry as an anti-freeze.
29 To our knowledge this is the first report on its response to stress in plants. The identified metabolites
30 and candidate genes provide novel targets for the development of heat tolerant wheat.

34 **Key words**

35 Climate resilient crops, heat stress, wheat, secondary metabolites, ROS, antioxidants, photosynthesis,
36 propanediol

37

38

39 **Overview of manuscript:**

40 **Tables and figures:**

41 **Table 1:** Annotated genes showing a cultivar-specific heat response.

42 **Table 2:** Genes with constitutive differential genotypic expression

43 **Figure 1** Phenotypic responses of two wheat varieties to different growth temperatures.

44 **Figure 2** Principal component analysis of phenotypic data.

45 **Figure 3** Heat map cluster analysis of metabolites.

46 **Figure 4** Heat-responsive metabolites, propanediol, DIBOA and dhurrin.

47 **Figure 5** Heat responsive metabolites of the flavonoid pathway.

48 **Figure 6** Heat-responsive metabolites of the phenylpropanoid pathway.

49 **Figure 7** RNAseq data analysis.

50 **Figure 8** Chemical radical scavenging and photosynthesis under heat stress.

51

52 **Supplemental Data:**

53 Figure S1. Phenotypic data Cadenza and Paragon at five different Tmax

54 Figure S2. Plant height and tiller number of plants harvested for RNAseq and metabolomics

55 Figure S3. Metabolite raw data transformed

56 Table S1. NMR metabolite list and statistical analysis

57 Table S2. LCMS metabolites list and statistical analysis

58 Table S3. Average p values across three time points of LCMS and NMR metabolites

59 Table S4. LCMS and NMR raw data

60 Table S5. Full list of DEGs, annotated

61 Table S6. Genotype-specific DEGs, annotated

62 Table S7. Genotype-specific genes, GO terms

63 Table S8. Heat responsive DEGs, GO term and genes within

64 Table S9. Genotype x temperature interaction DEGs, full list, annotated

65

66 INTRODUCTION

67 The global average temperature had increased by nearly 1°C above pre-industrial levels in 2017, and
68 unprecedented measures would be needed globally to limit further warming to 1.5°C (Masson-
69 Delmotte et al., 2019). Climatic changes cause increasingly severe, erratic weather events, such as
70 droughts, floods, and heat waves. Based on a recent comparative modelling study, it is estimated that
71 each 1°C increase in average temperature will cause significant yield losses, most severely affecting
72 maize (-7.4%) and wheat (-6.0%), followed by rice (-3.2%) and soybean (-3.1%) (C. Zhao et al., 2017).

73 The development of climate resilient crops is thus a matter of global food security.

74 High T stress affects every aspect of plant performance, including changes in phenology, growth and
75 development, and yield. During the reproductive phase, high T causes pollen sterility and failure of
76 fertilization and seed set (e.g., (Erena et al., 2021; Jagadish et al., 2010), whilst post-anthesis heat
77 stress negatively effects grain size and quality in crops, such as rice (e.g., (Yan et al., 2021) and wheat
78 (X. Wang & Liu, 2021). The negative impact of high temperatures has been shown for most
79 economically important crops, including maize, barley, tomato, peanut, potato, rapeseed, grapes,
80 citrus and others (for a review see Janni et al., 2020).

81 The detrimental effect of vegetative heat stress on grain yield has been shown in a recent genetic
82 diversity study in rice, with intolerant genotypes showing up to eighty percent yield reduction (Cheabu
83 et al., 2018). However, the study also indicated that there are opportunities for tolerance breeding,
84 since yield reduction in some genotypes was only thirty percent. An extensive comparative study in
85 wheat using more than one hundred genotypes adapted to rain-fed conditions has shown a thirty
86 percent reduction in tiller number, and this was associated with a significant reduction in SPAD values,
87 as an indicator for chlorophyll content (Qaseem et al., 2019).

88 Most studies on heat stress are being conducted exposing plants to very high temperatures (37-47°C
89 for rice, 35-42°C for wheat), usually for a short period of time during the reproductive stage (for a
90 review see (Janni et al., 2020). However, studies on the effect of high night-time temperatures (HNT)
91 have made it clear that relatively mild heat stress can cause significant yield losses. For instance, a
92 diversity field study in rice showed significant yield losses when night T were raised by as little as 1-
93 3°C above ambient (Xu et al., 2021) and this was also observed in wheat (Prasad et al., 2008). Yield
94 losses due to HNT in rice and wheat have been associated with enhanced night-time respiration and
95 decrease in grain starch (Impa et al., 2019, 2020; Xu et al., 2020).

96 The negative impact of heat stress on photosynthesis has been investigated in many studies (for a
97 review see Hu et al., 2020) and the stay-green phenotype has been associated with tolerance in wheat
98 (Shirdelmoghanloo et al., 2016), as well as in sorghum and other crops (for a review see Kamal et al.,

99 2019). Recent work in wheat has demonstrated the important role of Rubisco and Rubisco activase
100 (*Rca*) under heat stress; the identification of *Rca* alleles with higher thermotolerance holds promise
101 for the development of crops that maintain photosynthesis under heat stress (Degen et al., 2020a;
102 Perdomo et al., 2017; Scafaro et al., 2019). High T increases fluidity of membranes which, in
103 chloroplasts, leads to dissociation of the photosystem II (PSII) light-harvesting complex from thylakoid
104 membranes disrupting electron transfer and increasing formation of reactive oxygen species (ROS),
105 such as reactive singlet oxygen (Dogra & Kim, 2019; S. Hu et al., 2020a; Sun & Guo, 2016). Singlet
106 oxygen, as well as other ROS, such as H₂O₂ or O₂⁻ and OH[·] produced in the chloroplast, mitochondria
107 and other plant organelles, increase under stress. This causes damage to DNA and membranes due to
108 lipid peroxidation, as well as oxidation of proteins, ultimately leading to cell death (Das &
109 Roychoudhury, 2014). Hence, photo-protection and antioxidants have been recognized as a key
110 component for developing heat tolerant wheat (Cossani & Reynolds, 2015).

111 Plants have evolved a range of mechanisms to maintain ROS homeostasis, including enzymatic ROS
112 scavenging by e.g., superoxide dismutase (SOD), catalase, ascorbate peroxidase (APX) or glutathione
113 reductase (GR). In addition, chemical, non-enzymatic ROS scavenging is facilitated by e.g., ascorbic
114 acid and reduced glutathione, as well as tryptophane-derived molecules generated within the
115 flavonoid and phenylpropanoid pathways (Das & Roychoudhury, 2014; Hasanuzzaman et al., 2020).
116 The latter represent a tremendously diverse group of phenolic molecules, of which many have shown
117 ROS scavenging and anti-cancer properties (Kopustinskiene et al., 2020). In addition to the antioxidant
118 pathways, plants possess a suite of protective molecular chaperones, including large gene families of
119 heat shock proteins (HSPs), such as HSP70 and HSP90, as well as small HSPs. In wheat, a total of 753
120 HSP genes were identified, including 169 sHSPs, 114 HSP70s, and 18 HSP90s (A. Kumar et al.,
121 2020b). The best characterized regulatory pathway responsible for upregulation of HSPs under heat
122 stress is ROF1 (Meiri & Breiman, 2009), which enables nuclear import of the transcription factor
123 HSFA2A, a positive regulator of sHSP gene expression, dependent on interaction with HSP90 and
124 FKBP62 (a peptidyl prolyl cis/trans isomerase).

125

126 To further enhance our understanding of plant heat adaptation during vegetative growth, we have
127 conducted a chronic heat-stress experiment using two UK spring wheat varieties that differ in their
128 phenotypic response to high temperature stress. RNAseq and metabolomics analysis of vegetative
129 tissue, collected pre-dawn and in the afternoon, revealed a set of interesting gene candidates and
130 novel heat-responsive metabolites highlighting the importance of maintenance of photosynthesis and
131 radical scavenging.

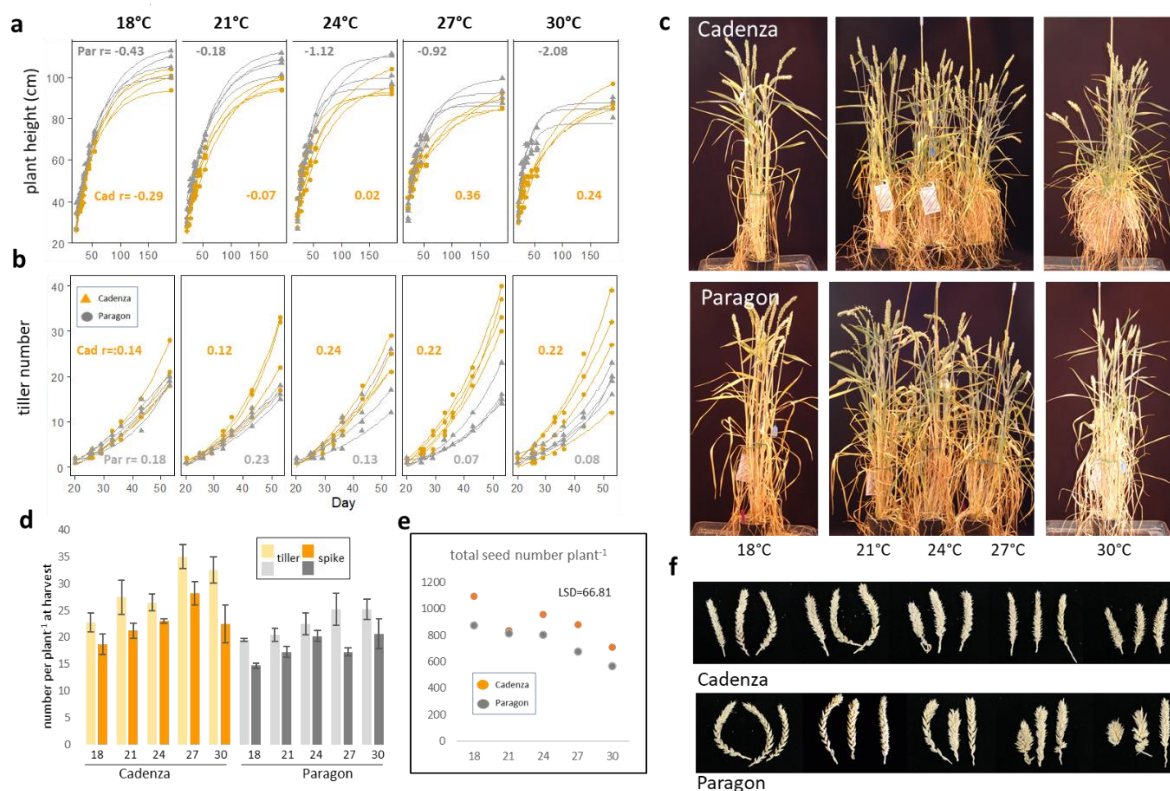
132

133 **Results**

134 **Phenotypic effect of heat treatment**

135 The two UK bread wheat genotypes included in this study both responded to high temperatures with
136 a reduction in plant height (PH), with Paragon showing a significant change in growth rate at 24°C
137 whilst this occurred at 27°C in Cadenza (Figure 1a). At plant maturity, PH at T_{max} 30°C compared to
138 18°C, was reduced by 24.3% in Paragon (from avg. 107.0 cm to 81.0 cm) and by 10.0% in Cadenza
139 (from avg. 99.7 cm to 89.0 cm) (Suppl Figure S1). In contrast, tiller number (TN) significantly ($p < 0.05$)
140 increased under heat stress in both genotypes (Figure 1b). This was most pronounced in Cadenza at
141 T_{max} 27°C and 30°C with an avg. tiller number of >32 compared to avg. 23 tillers at 18°C. This
142 corresponds to 43-54% heat-induced increase in tiller number (Suppl Figure S1). In Paragon, TN under
143 heat increased by 30% (from avg. 19.5 at 18°C to 25.3 at 30°C). Representative plants at the harvesting
144 stage are shown in Figure 1c.

145 In agreement with the observed increase in TN under heat stress, the number of fertile tillers and thus
146 spikes remained higher, although both genotypes aborted some tillers (Cadenza avg. 3.5-10; Paragon
147 2.3-8.0) (Figure 1d). In Cadenza, the highest spike number was found at T_{max} 27°C with an avg. of 28.3
148 spikes, a 50.5% increase over an avg. 18.8 spikes at 18°C. At T_{max} 30°C, spike number declined but was
149 still higher by an avg. 3.7 spikes compared to 18°C (Figure 1d). Likewise, in Paragon spike number
150 under heat was increased (by avg. 2.5 spikes at 27°C, 16.0 %; avg. 5.9 at 30°C, 39.9 %) (Figure 1d; Suppl
151 Figure S1).



152

153 **Figure 1. Phenotypic responses of two wheat varieties to different growth temperatures.**

154 *Cadenza and Paragon plants were grown at the indicated five different Tmax. Models were fitted to*
 155 *describe changes over time in plant height (a, negative r = slower exponential growth rate) and tiller*
 156 *number (b, r = gradient of growth). Representative plants at maturity are shown in c. Tiller number*
 157 *and spike number are shown in d. Total seed number per plant and representative spikes are shown in*
 158 *e and f.*

159

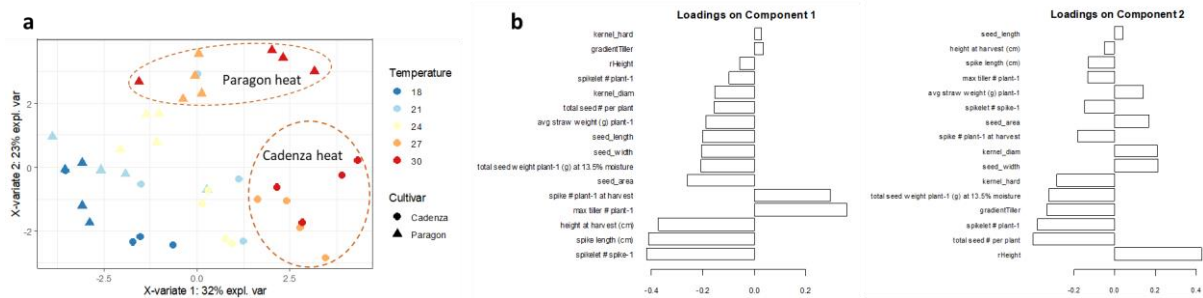
160

161

162 In contrast, spike length significantly decreased with increasing T (Suppl Figure S1). Overall, this was
 163 less pronounced in Cadenza with a reduction of 34% (avg. 12.9 cm, 18°C to 8.52 cm, 30°C) compared
 164 to 46.8% reduction in Paragon (from avg. 15.6 cm to 8.3 cm). This corresponded to a significant
 165 reduction in spikelet number per spike which again was less severe in Cadenza (40% reduction)
 166 compared to Paragon (50%) (Suppl Figure S1). However, due to the higher number of spikes in
 167 Cadenza, the total spikelet number and seed number per plant was significantly higher across all
 168 temperatures, with an average of 315 spikelets and 708 seeds per plant at 30°C in Cadenza compared
 169 to avg. 280 spikelets and 492 seeds in Paragon (Figure 1e; Suppl Figure S1). Compared to 18°C, this
 170 corresponds to a reduction in seed number per plant by 35.2% in Cadenza and 43.8% in Paragon.
 171 Accordingly, total seed weight was reduced by only 33.1% in Cadenza (from avg. 49.6g to 33.2g) but

172 44.5% in Paragon (from avg. 45.4 to 25.2g) (Suppl Figure S1). Representative spike images are shown
 173 in Figure 1f. There was no significant effect of the temperature treatment on seed parameters, such
 174 as seed size, area and hardness in either genotype (Suppl Figure S1).
 175 The above data suggest a differential heat response, and this was confirmed by a PCA analysis (Figure
 176 2a, b), which distinguished between the five different temperatures and clearly separated Paragon
 177 and Cadenza at T_{max} 27°C and 30°C, based on the higher number of spikes and yield observed in
 178 Cadenza.

179



180

181 **Figure 2. Principal component analysis of phenotypic data.**

182 *The principal component analysis separated Paragon and Cadenza at T_{max} 27°C and 30°C (a). The*
 183 *loadings for components 1 and 2 are shown in (b). The actual data are provided in the Supplemental*
 184 *Figure 1.*

185

186

187

188 **Molecular characterization of the differential heat response in spring wheat**

189 To determine the molecular mechanisms behind the observed genotypic differences, an additional set
 190 of plants were grown at T_{max} 21°C/15°C and 27°C/21°C (day/night) and sampled for RNAseq and
 191 metabolomics analyses. Pre-dawn (AM) leaf samples were analysed to assess the effect of high night-
 192 time T, whereas afternoon (PM) samples were analysed to assess response to acute heat stress.

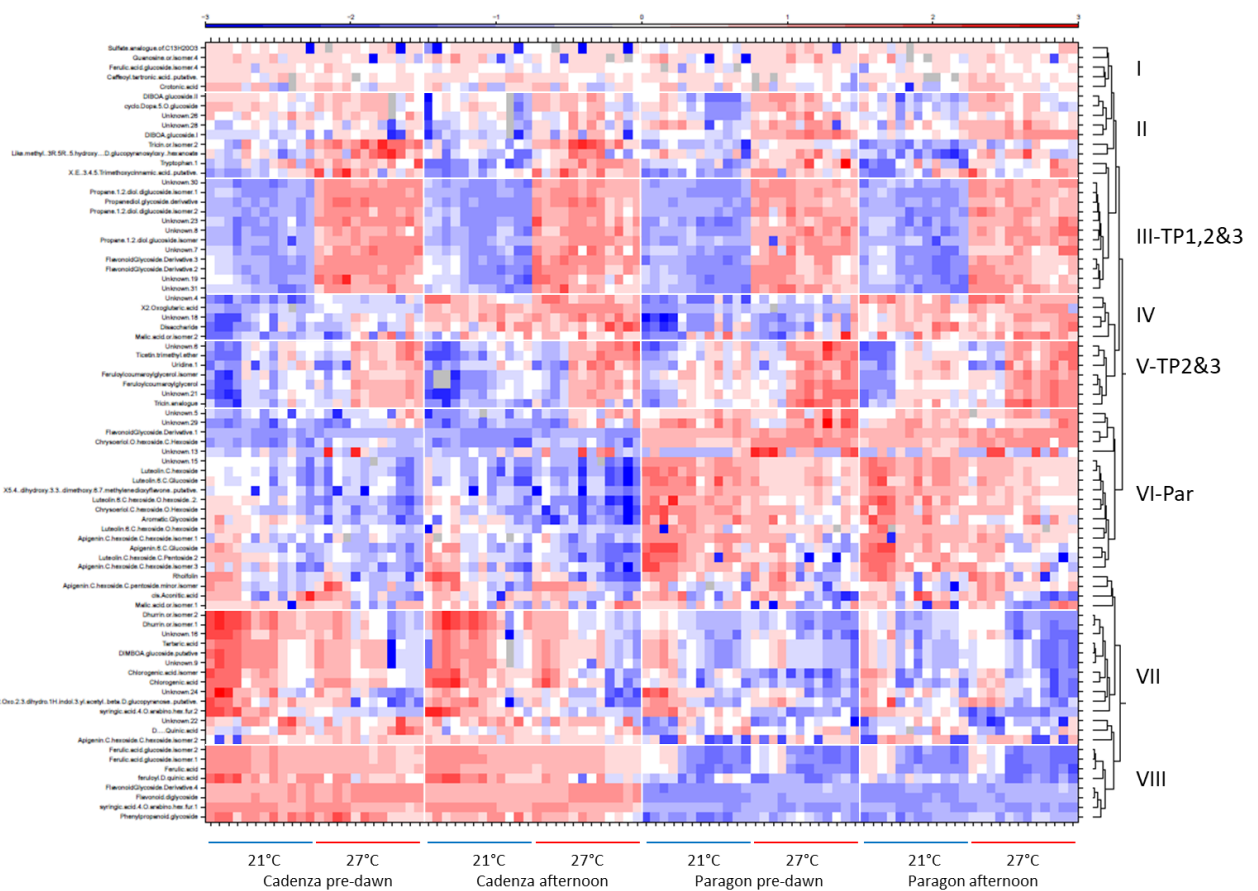
193 Targeting the causal factors of differential heat response, plants were sampled at three developmental
 194 stages (26-47 days post germination; TP1, TP2, TP3) before heat-induced changes in plant
 195 development became apparent (Suppl Figure S2).

196

197 **Metabolite analysis**

198 Primary metabolites, including mainly amino acids and sugars, were found to be largely unresponsive
 199 to the temperature treatment and to the time-of-day of sampling (Suppl. Table S1). A significant
 200 response to heat was observed only for asparagine and glutamate at TP1 and TP2, and for glutamine

201 at TP1, pre-dawn and in the afternoon. Proline, a small amino acid often reported to be upregulated
 202 under stress, showed a significant heat response only at TP1, pre-dawn (Suppl. Table S1).
 203 In contrast, a number of secondary metabolites showed a significant response to heat (Suppl. Table
 204 S2). Based on a cluster analysis, eight distinct groups were identified (Figure 3), of which groups II and
 205 III contain metabolites that are heat responsive at pre-dawn and in the afternoon at all three time
 206 points, whereas group V was heat responsive only at TP2 and TP3. Metabolites in group IV were not
 207 heat-responsive and were PM specific. The remaining groups contained metabolites specific to
 208 Paragon (group VI) and Cadenza (VII, VIII), respectively, indicating constitutive differences in metabolic
 209 pathways between these two spring wheat genotypes. Large constitutive differences were also
 210 observed in the RNAseq analysis (see below).

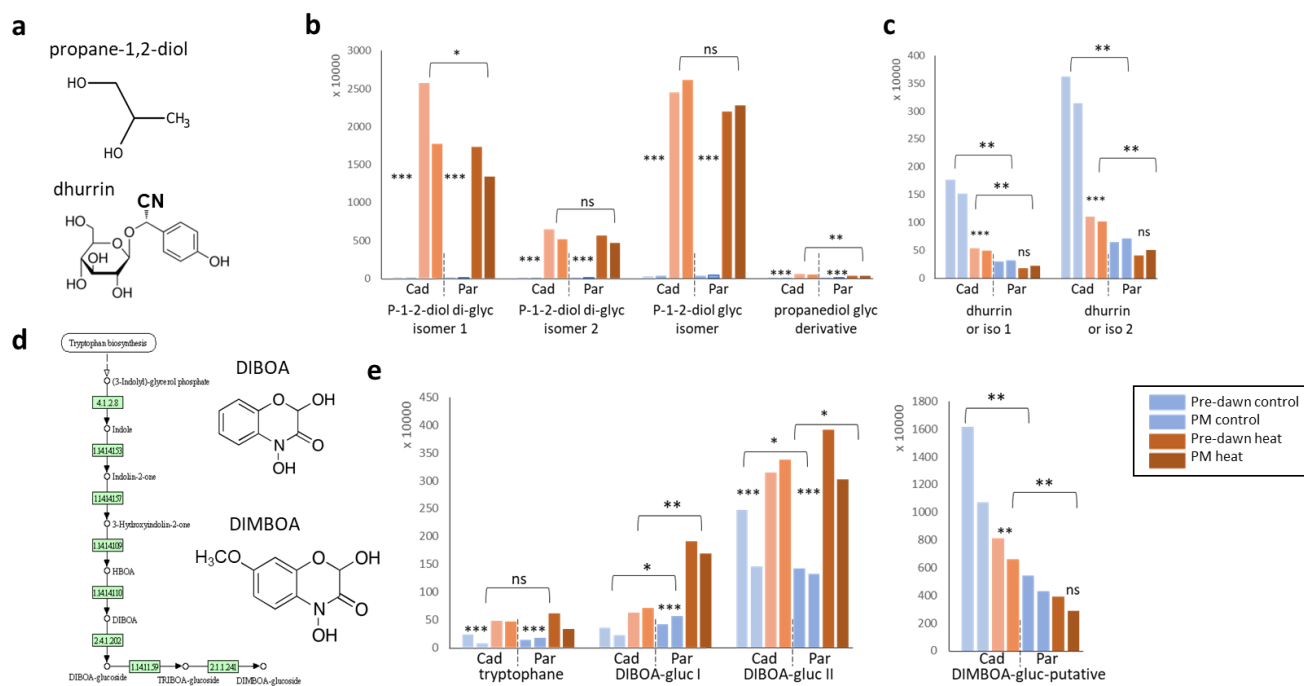


211
 212 **Figure 3. Heat map cluster analysis of metabolites.**

213 *Leaf samples were collected pre-dawn and in the afternoon from Cadenza and Paragon plants at T_{max}*
 214 *21°C and T_{max} 27°C. For each T_{max} , three developmental stages with four replicates each are included*
 215 *(not indicated; see main text for details). The clusters were manually re-assessed and grouped into the*
 216 *eight groups indicated to the right. The actual data are provided in the Supplemental data Table S1*
 217 *and Table S2.*

219
 220
 221
 222
 223
 224
 225
 226
 227
 228
 229
 230
 231
 232
 233

For simplicity, average values across the three analyzed time points are presented in Figures 4-6. Statistical analysis and NMR and LCMS raw data are provided in the supplemental data (Suppl. data Tables S2-S4) Amongst the most highly heat-induced molecules in both genotypes and part of group III was propane-1,2-diol (P-1,2-diol) and glycosylated derivatives (Figure 4a, b). The highest increase was observed for P-1,2-diol di-glucoside isomer 1, which increased by up to 390-fold in Cadenza and 480-fold in Paragon, when averaged across the three time points (Figure 4b). Similarly, the di-glycoside isomer 2 increased up to 180-fold in Cadenza and 190-fold in Paragon, whilst a mono-glycosylated P-1,2-diol isomer and a low-abundant isomer increased to a lesser extent (85 and 44-fold in Cadenza, 57 and 19-fold in Paragon, respectively). Propane-diol is a small molecule (Figure 4a) widely used in the food and cosmetic industry as an emulsifier and anti-freeze compound, enhancing viscosity of liquids. Despite its industrial value, the role and biosynthesis pathway in plants are not established and we were unable to find any detailed information apart from that it might be synthesized from glycerone-P, a glycolysis compound (KEGG pathway map00640; propanoate metabolism).



234
 235
 236
 237
 238
 239
 240

Figure 4. Heat-responsive metabolites, propanediol, DIBOA and dhurrin.

The chemical structure (a) and abundance of propane-1,2-diol (b) and dhurrin (c) for simplicity averaged across the analysed three developmental stages is shown. The actual data are provided in the Supplemental data Table S1 and S2. The blue bars indicate control growth conditions at 21°C pre-dawn (left) and afternoon (right). The brown bars indicate growth at 27°C pre-dawn (left) and PM (right). Two metabolites of the benzoxazinoid pathway, DIMBOA and DIBOA and their average

241 *abundance are shown in d and e. Note that the aglycons are shown here. Cad = Cadenza; Par =*
242 *Paragon. Asterisks *, **, *** indicate significant difference at $p < 0.05$, 0.001 and 0.0001*
243 *(Supplemental Table S3). Ns = non-significant.*

244

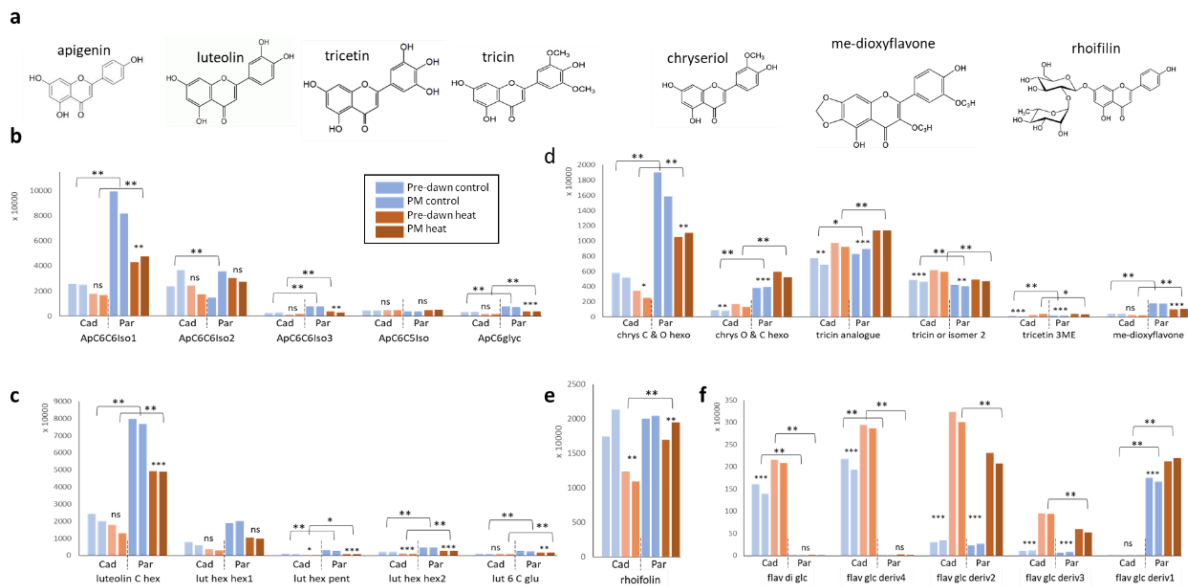
245

246 Another interesting molecule identified in this study is dhurrin (isomer 1 and 2; group VII), which, in
247 contrast to propane-diol, was downregulated under heat stress (Figure 4a, c). This was more
248 pronounced in Paragon (up to 71-fold reduction) compared to Cadenza (3-fold reduction) and because
249 both dhurrin isomers were more abundant in Cadenza under control conditions they remained
250 significantly higher (about 2-fold) under heat stress in Cadenza compared with Paragon. Dhurrin is a
251 cyanogenic aromatic glucoside due to the presence of a CN chemical group (Figure 4a) which can form
252 highly toxic cyanides. However, recently dhurrin has been discussed as a possible N source (Bjarnholt
253 et al., 2018; Rosati et al., 2019). Interestingly, putative cyanide-detoxifying rhodanese-domain
254 containing genes (Hatzfeld & Saito, 2000) have been identified in the RNAseq data and showed
255 expression specific to Paragon (TraesCS6A02G005800, TraesCS7D02G531600, TraesCS6A02G005800)
256 or pre-dawn (TraesCS6A02G106000, TraesCS5A02G315800, TraesCS5B02G316400) (see below).

257 Amongst the molecules in the heat-responsive group II was glycosylated DIBOA (2,4-Dihydroxy-1,4-
258 benzoxazin-3-one) and its methoxylated derivative DIMBOA (putative) (Figure 4d, e). These molecules
259 represent aromatic benzoxazinoids derived from tryptophane and are well known for their
260 importance in plant defence acting as a natural pesticide (see discussion). In both, Cadenza and
261 Paragon, this pathway was differentially regulated with a heat-induced two- to six-fold increase in
262 tryptophane and a corresponding increase in DIBOA glycoside I and II (between 1.2 and 4.5-fold). In
263 contrast, DIMBOA glycoside, which is further downstream in the pathway (Figure 4d), was
264 downregulated under heat stress but remained significantly (about 2-fold higher) under heat stress in
265 Cadenza compared to Paragon, as was observed for dhurrin (Figure 4e). In agreement with that, the
266 RNAseq data (see below) revealed constitutively higher expression of the DIMBOA UDP-
267 Glucosyltransferase gene BX8 (PTHR11926:SF1486; TraesCS7A02G344300) in Cadenza. On the other
268 hand, two genes encoding DIMBOA glucosidases (TraesCS5B02G294600, TraesCS5A02G295200)
269 increased significantly under heat in both genotypes. Additional DIMBOA glucosyltransferase genes
270 showed genotype-specific expression, with higher expression in Paragon (TraesCS2D02G522600, only
271 pre-dawn) or Cadenza (TraesCS7A02G389200, TraesCS2B02G599800) (see below).

272 Apart from the above, different molecules of two well-known plant pathways were identified, namely
273 the phenylpropanoid (KEGG map00940) and flavonoid (KEGG map00941) pathways.

274 Overall, the flavonoid pathway appeared more active in Paragon. Specific glycosylated isoforms of
 275 apigenin, luteolin and the tricetin precursor chrysoeriol (C-hexoside O-hexoside) were highly abundant
 276 and about 3-fold higher in Paragon compared to Cadenza (Figure 5a-d). Due to this, although generally
 277 downregulated under heat stress, they remained significantly higher in Paragon (up to 3.8-fold). This
 278 was also the case for less abundant luteolin and apigenin isoforms (Figure 5b, c). Another highly
 279 abundant molecule was rhoifilin, a glycosylated apigenin derivative, which was also showed lower
 280 abundance under heat stress but remained significantly higher in Paragon (Figure 5a, e). Other
 281 metabolites of the flavonoid pathway were positively heat-responsive in both genotypes. This was the
 282 case for tricetin-related molecules (tricetin analogue, tricetin or isomer 2) and tricetin, as well as a putative
 283 di-methoxy flavone (Figure 5a, d). Chrysoeriol appears to be differentially glycosylated and contrary
 284 to the above-mentioned C-O glycosylated isoform, the O-hexoside C-hexoside isoform was
 285 significantly upregulated under heat stress in both genotypes and more abundant in Paragon (Figure
 286 5d). Lastly, a group of unspecified glycosylated flavonoids was significantly more abundant under heat
 287 stress (up to 40% increase) (Figure 5f). Whilst some derivatives were specific to Cadenza (flavonoid-di-
 288 glycoside, derivative 4) or Paragon (derivative 1), others were heat-responsive in both genotypes but
 289 significantly more abundant in Cadenza (derivative 2 and 3) (Figure 5f).
 290
 291



292

293 **Figure 5. Heat responsive metabolites of the flavonoid pathway.**

294 The chemical structures (aglycons) of the identified flavonoid metabolites are shown in (a). Average
 295 values are shown as described in the legend of Figure 4 for apigenin-derived molecules (b) and luteolin-
 296 derivatives (c). Chryseriol derivatives and tricetin derivatives, and a methoxy-dioxyflavone is shown in (d)
 297 and rhoifilin in (e). A highly heat induced unspecified differentially glycosylated flavonoid is shown in

298 (f). *Cad*= Cadenza; *Par* = Paragon. Asterisks *, **, *** indicate significant difference at $p < 0.05$, 0.001
299 and 0.0001 (Supplemental data Table S3). *Ns*= non-significant.

300

301

302

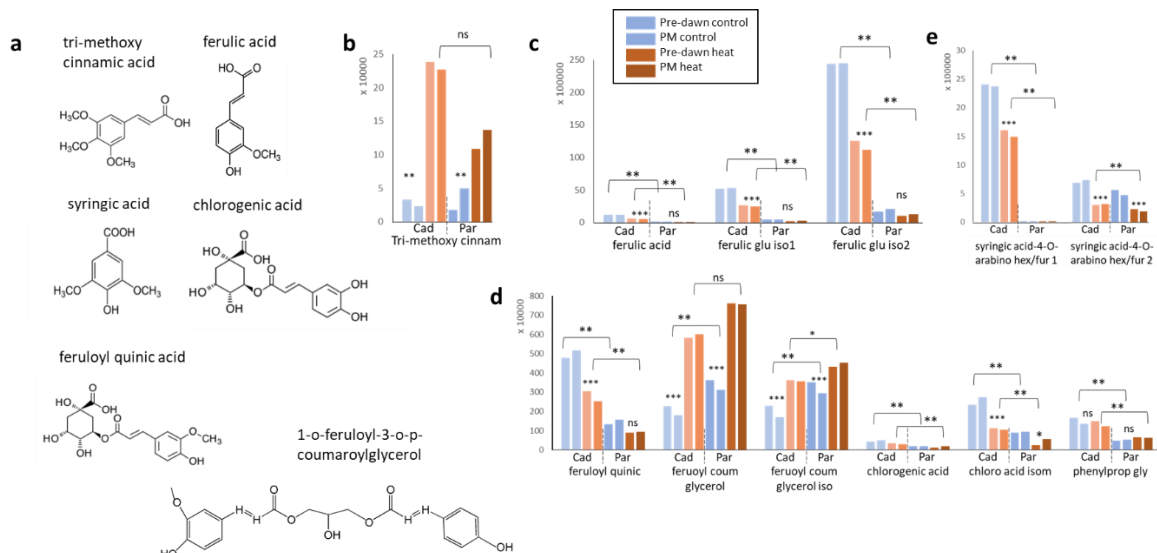
303

304 As was observed for the flavonoids, metabolites of the phenylpropanoid pathway were mostly
305 downregulated under heat stress and showed quantitative differences between the genotypes (Figure
306 6a-e). No genotypic difference or significant heat response was detected for phenylalanine, the pre-
307 cursor of the phenylpropanoid pathway (suppl data Table S1). Cinnamic acid is the first compound in
308 this pathway, and we found a significant increase in tri-methoxy cinnamic acid under heat stress to
309 about the same level in both genotypes, though there was a higher fold change in Cadenza (7- to 9.6-
310 fold) compared with Paragon (3- to 6-fold) (Figure 6b). Ferulic acid, which is further downstream in
311 this pathway and two more abundant glycosylated isoforms were downregulated under heat stress
312 but remained significantly higher in Cadenza (by 8.5 to 12-fold; Figure 6c). Likewise, related feruloyl-
313 D-quinic acid was reduced under heat stress but remained about 3-fold higher in Cadenza (Figure 6d).
314 Contrary to this, a positive heat response was observed for feruloyl-coumaroylglycerol and an isomer,
315 which significantly increased in both genotypes by up to 2-fold (Figure 6d). Other phenylpropanoid-
316 related molecules, chlorogenic acid and an unspecified glycosylated phenylpropanoid, were less
317 abundant and reduced under heat stress, but again remained higher in Cadenza (Figure 6d). This was
318 also the case for two syringic acid-related molecules of which syringic acid-4-O-arabino hex/fur 1 was
319 12-14-fold higher under heat stress in Cadenza compared to Paragon (Figure 6e).

320 Taken together the data showed that the flavonoid and phenylpropanoid pathways are highly
321 responsive to heat stress, either negative or positive, and display genotype-specific differences in
322 abundance and glycosylation pattern. Overall, the latter appeared more active in Cadenza whereas
323 the flavonoid pathway appeared more responsive in Paragon. It is noteworthy, that phenylpropanoids
324 with methoxy groups (-OCH₃) were overall more abundant in Cadenza (Figure 6a).

325

326



327

328 **Figure 6. Heat-responsive metabolites of the phenylpropanoid pathway.**

329 The chemical structures (aglycons) of the identified phenylpropanoid metabolites are shown in (a).

330 Average values are shown as described in the legend of Figure 4 for Tri-methoxy-cinnamic acid (b),

331 ferulic acid and its glucosylated derivatives (c). Derivatives of ferulic acid and chlorogenic acid are

332 shown in (d) and derivatives of syringic acid are shown in (e). Cad= Cadenza; Par = Paragon. Asterisks

333 *, **, *** indicate significant difference at $p < 0.05$, 0.001 and 0.0001 (Supplemental data Table S3).

334 Ns= non-significant.

335

336

337 RNAseq analysis

338 The same samples used for metabolomics analysis were used for gene expression analysis by RNAseq.

339 A PCA analysis of the DEG data set showed a clear separation of the two genotypes (57% of variance)

340 and time-of-day of sampling (AM, PM; 28% of variance), as well as a small effect of temperature, whilst

341 the three analysed developmental stages showed little separation (Figure 7a). In total, 6023 genes

342 were differentially expressed, either due to heat treatment, cultivar, or an interaction between the

343 two (Fig. 7b, c; Suppl Table S5). There were more than 5500 genes that showed a differential

344 expression between Paragon and Cadenza, independent of the treatment, suggesting substantial

345 genotypic differences despite both being modern spring wheats (Figure 7d; Suppl. Tables S6 and S7).

346 A total of 404 genes were temperature-responsive in both cultivars and 44 of these DEGs were

347 differentially expressed pre-dawn and PM (Figure 7e; Suppl. Table S8). This group includes a large

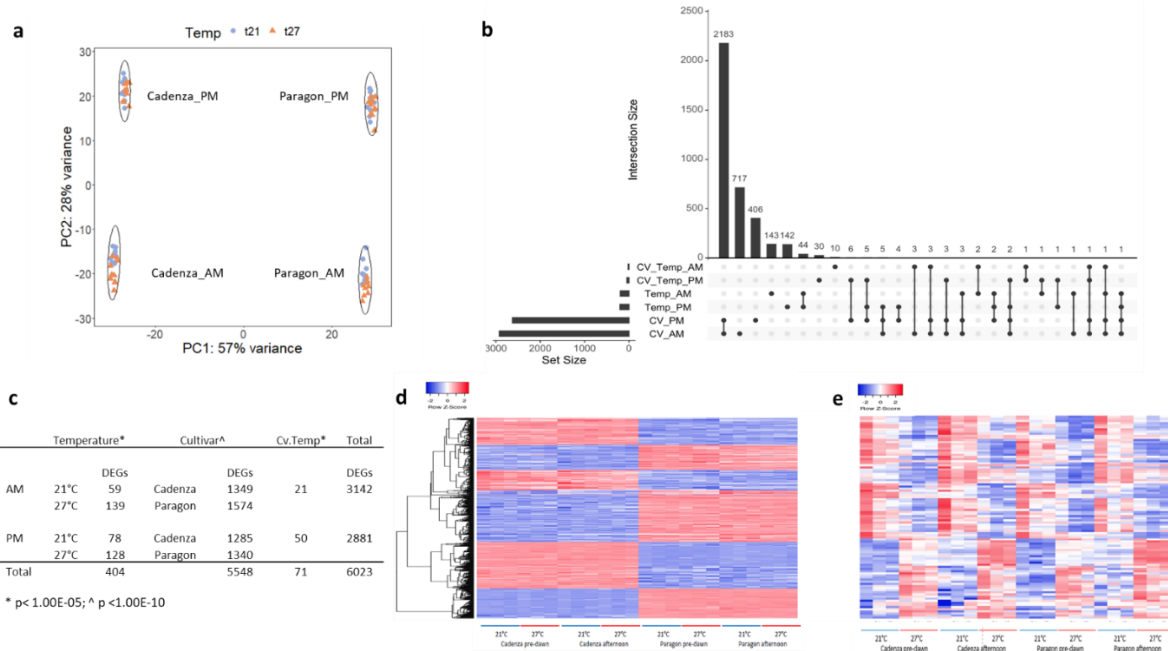
348 number of HSPs and other known heat-responsive genes (see below), which is indicative of the

349 effectiveness of the heat treatment applied in this study.

350 The majority of the genes in the genotype x temperature interaction group were found in the

351 afternoon, indicating a genotype-specific response to exposure to acute heat stress, because T_{max} was

352 reached during the day. There was very little overlap between the temperature and cultivar DEGs
 353 (Figure 7b), and only 71 genes (53 annotated genes; Figure 7c; Suppl. Table S9) showed an interaction
 354 between the two factors at the thresholds applied. These genes are the most relevant for this study
 355 since they might help to explain the observed different levels of heat tolerance between the two
 356 genotypes.
 357



358 **Figure 7. RNAseq data analysis.**
 359 *A principal component analysis of the differentially expressed genes (DEGs; a) clearly separated the*
 360 *two genotypes Cadenza and Paragon and the time-of-day of sampling (pre-dawn and afternoon).*
 361 *Within that, a temperature effect is evident, though to a lesser extent. The number of temperature*
 362 *responsive DEGs, genotype specific DEGs and DEGs that showed an interaction is shown in the upside-*
 363 *down plot (b) and corresponding table (c). The cluster analysis heat map shown in (d) illustrates the*
 364 *genotype-specific genes and the heat map in (e) shows the heat-responsive genes. See legend of Figure*
 365 *3 for details. Details on the DEGs are provided in Table1 and 2, and Supplemental data Tables S5-9.*
 366

367
 368
 369

370 Genotype x temperature interaction genes

371 Amongst the most heat-responsive group of genes were those coding for protein chaperones (Table
 372 1; Suppl. Table S9). For example, two dehydrins, belonging to the Late Embryo Abundant family of
 373 disordered chaperones, showed large (log2 8-19) fold changes, and showed increased transcript
 374 abundance under heat in Cadenza whilst expression decreased in Paragon. Other differentially

375 expressed chaperones include HSP70s (TraesCS6D02G049100, TraesCS6B02G058300,
376 TraesCS6A02G042600), HSP100s, a HSP60 (TraesCS4A02G409100), and a small HSP
377 (TraesCS7A02G232500). Expression of the HSP genes was found to increase more in Paragon than
378 Cadenza under heat suggesting that Paragon experienced a higher level of stress. However, expression
379 of two HSP70s (TraesCS6B02G058300 and TraesCS1A02G295600) was overall higher in Cadenza under
380 both heat and control conditions (Suppl. Table S9). A cold shock protein (TraesCS6A02G350100;
381 CS120), which decreased expression in Paragon under heat, remained stable in Cadenza.

382 Three genes related to lipid metabolism were differentially expressed, suggesting that heat treatment
383 had an impact on membrane integrity. These genes included two homoeologues of a lipase GDSL
384 domain-containing gene (TraesCS5A02G238300 and TraesCS5B02G236800) and non-specific lipid-
385 transfer protein 2G (nsLTP protein 2G; TraesCS4B02G393300). Expression of all three genes were
386 overall higher in Paragon than Cadenza, but Cadenza demonstrated a greater (approx. 3-fold log₂)
387 upregulation under heat (Table 1; Suppl. Table S9). Three genes encoding Ankyrin repeat domain
388 containing proteins (TraesCS4A02G290200, TraesCS2B02G587800 and TraesCS4A02G290100), which
389 mediate protein-protein interactions, showed higher transcript abundance in Cadenza, and although
390 they increased in Paragon in response to heat, expression levels were still lower in the heat sensitive
391 cultivar (Table 1; Suppl. Table S9).

392 Other genes with a positive heat response in Cadenza included an F-box domain-containing protein
393 (TraesCS5B02G080800), which showed overall higher expression in Paragon but no increase under
394 heat. Likewise, an Aa_trans domain-containing protein showed a Cadenza-specific increased
395 expression (AM samples). A cysteine protease (TraesCS7B02G485300) showed overall higher
396 expression in Cadenza under both control and heat conditions and was positively heat responsive in
397 DS1. Similarly, a hypersensitive-induced response protein (TraesCS5B02G188800) showed an early
398 (DS1) positive heat responsive only in Cadenza. Two other genes with differential heat response
399 included an Aldo_ket_red domain-containing protein (TraesCS3A02G045300) and a peroxidase gene
400 (TraesCS6A02G324200). The former showed overall higher expression and positive heat response in
401 Paragon. In contrast, expression of the peroxidase gene was reduced in Paragon under heat, in both
402 AM and PM samples, whilst in DS1 in Cadenza, it was unchanged (AM) or showed increased expression
403 (PM) under heat. However, in the other samples, expression under heat was reduced also in Cadenza.

404 DEGs with roles in carbon partitioning, cell wall and hormone regulation were amongst the genotype
405 x temperature interaction genes. These included two homeologs of a bidirectional sugar transporter
406 SWEET which decreased under heat in Cadenza (AM and PM), whereas in Paragon, expression
407 remained unchanged in the AM but increased under heat in the PM. In contrast, a fructan-6-
408 exohydrolase showed a Cadenza-specific increase under heat stress in DS1 (AM and PM). Galactinol-

409 sucrose galactosyltransferase 2-related also showed an increase in Cadenza under HT in the PM
410 samples. Two homeologs of xyloglucan endotransglucosylase/hydrolase showed decreased
411 expression in Paragon under heat (AM). A generally lower expression and sharp decline under heat
412 stress in Paragon, particularly in DS3, was also observed for polysacc_synt_4 domain-containing
413 protein. In contrast, a dirigent gene showed a Paragon-specific increase under heat stress (AM). Two
414 homeologs of abscisic stress-ripening protein 5 showed differential expression especially in DS1, with
415 a reduced expression under heat stress in Paragon (AM and PM).

416 Further to this there was a variety of genes with other functions, most of which were positively heat
417 responsive in Cadenza (Table 1; Suppl. Table S9) but had no obvious relationship with heat.

418

419 *Table 1 Annotated genes showing a cultivar-specific heat response. Arrows (^ and v) indicate direction of expression*
 420 *change. Only DEGs with BaseMean over 10 were included. Negative log 2 fold change values indicate upregulation in*
 421 *Cadenza relative to Paragon under high temperature and vice versa.*

Gene ID	DE Time of day	Cadenza	Paragon	BaseMean	log2FoldChange	padj	Annotation
TraesCS5B02G236800	AM	^	v	17.25	-3.29	0.04	LIPASE_GDSL DOMAIN-CONTAINING PROTEIN (PTHR45648:SF4)
TraesCS5A02G238300	AM	^	-	48.06	-2.81	0.05	LIPASE_GDSL DOMAIN-CONTAINING PROTEIN (PTHR45648:SF4)
TraesCS4B02G393300	PM	^	-	152.09	-2.97	0.00	NON-SPECIFIC LIPID-TRANSFER PROTEIN 2G (PTHR33214:SF34)
TraesCS7A02G232500	PM	-	^	210.46	1.25	0.04	23.6 KDA HEAT SHOCK PROTEIN, MITOCHONDRIAL (PTHR46991:SF11)
TraesCS4A02G409100	PM	v	^	238.04	1.58	0.00	CHAPERONIN (PTHR45633:SF30)
TraesCS6D02G049100	PM	v	^	473.73	1.04	0.00	HEAT SHOCK 70 KDA PROTEIN BIP1-RELATED (PTHR19375:SF492)
TraesCS6B02G058300	PM	v	^	1020.43	1.00	0.03	HEAT SHOCK 70 KDA PROTEIN BIP1-RELATED (PTHR19375:SF492)
TraesCS6A02G042600	PM	v	^	2397.77	0.87	0.00	HEAT SHOCK 70 KDA PROTEIN BIP1-RELATED (PTHR19375:SF492)
TraesCS1A02G295600	PM	^	^^	123.32	1.95	0.01	70 KDA HEAT SHOCK PROTEIN (PTHR19375:SF493)
TraesCS1D02G284000	PM	^	^^	1745.43	1.30	0.00	HEAT SHOCK COGNATE 71 KDA PROTEIN (PTHR19375:SF395)
TraesCS1A02G285000	PM	~ (DS1)	^ (DS1)	1221.36	1.03	0.05	HEAT SHOCK COGNATE 71 KDA PROTEIN (PTHR19375:SF395)
TraesCS5B02G426700*	AM	^	v	17.59	-17.76	0.00	DEHYDRIN RAB15 (PTHR33346:SF33)
TraesCS5B02G426700*	PM	^	v	41.68	-8.36	0.03	DEHYDRIN RAB15 (PTHR33346:SF33)
TraesCS6A02G350500	PM	^	v	17.89	-19.02	0.00	DEHYDRIN RAB16B (PTHR33346:SF37)
TraesCS6A02G350100	PM	-	v	115.66	-2.35	0.00	COLD-SHOCK PROTEIN CS120 (PTHR33346:SF14)
TraesCS4A02G290200*	AM	-	^	266.54	1.93	0.00	ANK_REP_REGION DOMAIN-CONTAINING PROTEIN (PTHR46224:SF19)
TraesCS4A02G290200*	PM	-	^	389.36	2.24	0.00	ANK_REP_REGION DOMAIN-CONTAINING PROTEIN (PTHR46224:SF19)
TraesCS2B02G587800	PM	-	^	51.65	2.52	0.05	ANK_REP_REGION DOMAIN-CONTAINING PROTEIN (PTHR46224:SF44)
TraesCS4A02G290100	PM	-	^	61.22	1.33	0.04	ANK_REP_REGION DOMAIN-CONTAINING PROTEIN (PTHR46224:SF19)
TraesCS3A02G045300	AM	-	^	22.17	4.05	0.05	ALDO_KET_RED DOMAIN-CONTAINING PROTEIN (PTHR11732:SF209)
TraesCS5B02G080800	AM	^	-	169.51	-1.41	0.04	F-BOX DOMAIN-CONTAINING PROTEIN (PTHR32153:SF43)
TraesCS7B02G485300	AM	^	v	775.00	-1.76	0.01	CYSTEINE PROTEASE (PTHR12411:SF803)
TraesCS5D02G180000	PM	^	-	254.16	-0.97	0.04	AA_TRANS DOMAIN-CONTAINING PROTEIN (PTHR22950:SF645)
TraesCS5B02G188800	PM	^ (DS1)	~ (DS1)	106.64	-1.30	0.03	HYPERSENSITIVE-INDUCED RESPONSE PROTEIN-LIKE PROTEIN 2 (PTHR43327:SF17)
TraesCS6A02G324200	PM	~ (DS1)	v (DS1)	539.72	-1.11	0.03	PEROXIDASE (PTHR31235:SF333)
TraesCS7B02G160000	PM	v	^	59.23	2.83	0.03	BIDIRECTIONAL SUGAR TRANSPORTER SWEET11 (PTHR10791:SF196)
TraesCS7D02G263100	PM	-	^	73.32	2.37	0.04	BIDIRECTIONAL SUGAR TRANSPORTER SWEET11 (PTHR10791:SF196)
TraesCS2B02G594900	AM	^	-	69.81	-2.42	0.01	FRUCTAN 6-EXOXYDROLASE (PTHR31953:SF71)
TraesCS1D02G157000	PM	v	^	10.02	3.57	0.04	CYTOKININ DEHYDROGENASE 3 (PTHR13878:SF107)
TraesCS4D02G109500	PM	-	v	5279.00	-0.83	0.04	ABSCISIC STRESS-RIPENING PROTEIN 5 (PTHR33801:SF24)
TraesCS4B02G112000	PM	-	v	5103.46	-1.09	0.03	ABSCISIC STRESS-RIPENING PROTEIN 5 (PTHR33801:SF24)

422

423

TraesCS2B02G100800	AM	∨	^	580.89	3.17	0.03	DIRIGENT PROTEIN (PTHR46506:SF1)
TraesCS7A02G427100	AM	-	∨	337.54	-1.72	0.01	XYLOGLUCAN ENDOTRANSGLUCOSYLASE/HYDROLASE (PTHR31062:SF239)
TraesCS7D02G419400	AM	-	∨	1397.68	-1.94	0.01	XYLOGLUCAN ENDOTRANSGLUCOSYLASE/HYDROLASE (PTHR31062:SF239)
TraesCS3B02G545900	PM	-	∨	58.30	-1.89	0.03	POLYSACC_SYNT_4 DOMAIN-CONTAINING PROTEIN (PTHR31444:SF2)
TraesCS2A02G384600	AM	∨	^	323.03	1.15	0.05	4-HYDROXY-7-METHOXY-3-OXO-3,4-DIHYDRO- 2H-1,4-BENZOXAZIN-2-YL GLUCOSIDEBETA-D- GLUCOSIDASE (PTHR10353:SF191)
TraesCS7D02G107900	AM	-	∨	444.74	-1.35	0.00	N- HYDROXYCINAMOYL/BENZOYLTRANSFERASE, PUTATIVE-RELATED (PTHR31147:SF33)
TraesCS6A02G239600	AM	∨	-	75.8	2.57	0	ALDEHYDE DEHYDROGENASE (PTHR43570:SF21)
TraesCS5B02G166300	AM	∨	^	345.62	2.25	0.01	INDOLE-3-GLYCEROL-PHOSPHATE SYNTHASE (PTHR22854:SF14)
TraesCS2D02G189900	PM	∨	^	29.28	1.84	0.03	PROTEIN CHROMATIN REMODELING 35 (PTHR45821:SF1)
TraesCS6B02G277100	PM	∨	-	119.36	1.37	0.04	AAI DOMAIN-CONTAINING PROTEIN (PTHR31731:SF24)
TraesCS3B02G299800	PM	∨	-	716.35	1.03	0.04	GLUTAMINE AMIDOTRANSFERASE TYPE-2 DOMAIN-CONTAINING PROTEIN (PTHR11938:SF133)
TraesCS6D02G090400	PM	-	^	929.58	0.72	0.03	Chaperone (PTHR11073:SF44)
TraesCS1B02G320800	PM	∨	-	1066.24	0.68	0.03	TUBULIN BETA-5 CHAIN (PTHR11588:SF327)
TraesCS4D02G279300	PM	-	∨	771.87	-0.58	0.04	POX (Plant Homeobox) DOMAIN-CONTAINING PROTEIN (PTHR11850:SF139)
TraesCS2D02G027600	PM	^	-	470.08	-0.84	0.01	DIOX_N DOMAIN-CONTAINING PROTEIN (PTHR10209:SF718)
TraesCS3A02G113900	PM	^	-	2385.82	-1.07	0.04	GALACTINOL-SUCROSE GALACTOSYLTRANSFERASE 2-RELATED (PTHR31268:SF32)
TraesCS4B02G051000	AM	^	-	125.5	-1.08	0.03	HYDROLASE_4 DOMAIN-CONTAINING PROTEIN (PTHR11614:SF155)
TraesCS3B02G039700	PM	^	-	136.19	-1.22	0.03	ASPERGILLUS NUCLEASE S(1) (PTHR33146:SF21)
TraesCS5B02G518400	PM	^	-	95.04	-2.21	0.05	BHLH DOMAIN-CONTAINING PROTEIN (PTHR31945:SF47)
TraesCS1B02G281100	PM	-	∨	49.28	-2.23	0.03	PROTEIN KINASE DOMAIN-CONTAINING PROTEIN (PTHR24343:SF431)
TraesCS3A02G420900	PM	^	∨	18.95	-3.03	0.04	F2103.6 PROTEIN (PTHR31579:SF1)

424

425

426

427 **Common heat responsive genes and constitutive genotypic differences**

428 The transcriptional heat response common to both cultivars was largely related to prevention of
429 protein degradation and to detoxification. Amongst the positive heat-responsive genes were a
430 number of HSP70s, HSP80s and HSP100s, as well as four peptidylprolyl isomerase genes, which are a
431 component of the well-studied ROF heat-response pathway (Meiri & Breiman, 2009). Importantly, in
432 both genotypes thirteen genes annotated as glutathione transferases were upregulated, an essential
433 component of non-enzymatic ROS scavenging. In contrast, enzymes such as catalase, SOD or
434 peroxidases were not induced by the heat stress applied and there was a similar number of genes
435 specific to Cadenza and Paragon, respectively (Suppl. Table S5), suggesting that both genotypes have
436 a similar capacity for enzymatic ROS scavenging. Interestingly, a large number (11) of aldo-keto-
437 reductase domain-containing proteins showed higher transcript abundance under heat stress (AM

438 and PM; Suppl. Table S5). Aldo-keto reductases constitute a superfamily in plants implicated with
439 many processes, including detoxification of reactive aldehydes that form under stress due to lipid
440 peroxidation. Also induced under heat stress were fifteen glycosyltransferase genes and these genes
441 are of interest in relation to the observed glycosylation of the phenolic metabolites described above.
442 The most significant GO terms for the large number of genes that showed a constitutive difference in
443 expression between Cadenza and Paragon were related to phosphorus metabolic processes and
444 kinase activity, as well as DNA packaging (Suppl. Table S6). Interestingly, there were several hundred
445 protein kinase genes that showed differential expression between the two genotypes, suggesting
446 substantial differences in signalling and protein regulation. This is very interesting and warrants
447 further investigation, however, it is beyond the scope of this study.

448 Amongst the genes that showed high base mean expression (>500) and most significant differences
449 between the two genotypes were a number of chloroplastic and photosynthesis-related genes (Table
450 2). Of particular interest is the higher constitutive expression of the RubisCo small subunit in Cadenza
451 (TraesCS2B02G078900), as well as the PsbP domain containing protein (TraesCS4B02G003600). The
452 latter is required for PSII assembly and repair and for adaptation to changing light conditions (Che et
453 al., 2020). In this context it is noteworthy that, although there was no significant difference between
454 the genotypes, three orthologues of *Arabidopsis* rubisco activase were significantly higher expressed
455 under heat stress (TraesCS4A02G177600, TraesCS4D02G134900, TraesCS4B02G140200; Suppl Table
456 S5). The differences in these and other photosynthesis-related genes might be directly relevant for
457 the observed differences in photosynthetic capacity and between Cadenza and Paragon (see below).
458 Interestingly, one of the most highly expressed genes, which showed significantly higher expression
459 in Paragon, was a glutamine synthetase 2 (GS2) gene (TraesCS2D02G500600). One of the main roles
460 of chloroplastic GS2 is the reassimilation of photorespiratory ammonium.

461

462 *Table 2 Genes with constitutive differential genotypic expression. Negative log 2 fold change values indicate upregulation in*
 463 *Cadenza relative to Paragon and vice versa.*

higher in	Gene ID	Annotation (Panther subfamily)	AM		PM	
			base mean	log2 fold change	base mean	log2 fold change
Cadenza						
	TraesCS2B02G078900	RIBULOSE BIPHOSPHATE CARBOXYLASE SMALL SUBUNIT 1B, CHLOROPLASTIC-RELATED (PTHR31262:SF10)	558.92	-4.71	3429.25	-5.33
	TraesCS4D02G309000	PHEOPHORBIDE A OXYGENASE, CHLOROPLASTIC (PTHR21266:SF24)	848.41	-2.23	-	-
	TraesCS4B02G003600	PsbP domain-containing protein	801.47	-5.76	682.9	-6.16
	TraesCS6B02G063000	PROTEIN LOW PSII ACCUMULATION 3, CHLOROPLASTIC (PTHR34051)	585.03	-2.01	591.17	-2.22
	TraesCS7A02G137000	RIESKE DOMAIN-CONTAINING PROTEIN (PTHR21266:SF45)	-	-	533.48	-2.53
	TraesCS4B02G003000	ASCORBATE TRANSPORTER, CHLOROPLASTIC (PTHR11662:SF255)	-	-	557.09	-1.81
	TraesCS4B02G009800	5-AMINO-6-(5-PHOSPHO-D-RIBITYLAMINO)URACIL PHOSPHATASE, CHLOROPLASTIC (PTHR47108:SF1)	519.92	-6.24	-	-
	TraesCS6B02G058300	HEAT SHOCK 70 KDA PROTEIN BIP1-RELATED (PTHR19375:SF492)	870.05	-2.30	1020.43	-2.40
	TraesCS6A02G000700	HSC70-INTERACTING PROTEIN (PTHR45883:SF2)	749.08	-1.49	-	-
	TraesCS3B02G041900	TRYPTOPHAN SYNTHASE (PTHR43406:SF8)	-	-	772.08	-1.67
	TraesCS2B02G204500	3BETA_HSD DOMAIN-CONTAINING PROTEIN (PTHR10366:SF696)	-	-	515.79	-12.49
Paragon						
	TraesCS2D02G500600	GLUTAMINE SYNTHETASE 2 (PTHR20852:SF57)	8860.64	3.22	10158.82	2.9
	TraesCS2B02G133500	PHOTOSYSTEM I REACTION CENTER SUBUNIT N, CHLOROPLASTIC (PTHR36814:SF1)	5430.49	3.21	8040.33	2.98
	TraesCS1B02G317500	CHLOROPHYLL A-B BINDING PROTEIN, CHLOROPLASTIC (PTHR21649:SF150)	-	-	6820.14	4.65
	TraesCS2A02G590600	PROTOCHLOROPHYLLIDE REDUCTASE A, CHLOROPLASTIC (PTHR44419:SF6)	-	-	6343.22	1.22
	TraesCS7D02G553300	PHYTOENE SYNTHASE, CHLOROPLASTIC (PTHR31480:SF2)	1348.03	9.37	1043.81	8.59
	TraesCS7B02G486500	PHOTOSYSTEM II STABILITY/ASSEMBLY FACTOR HCF136, CHLOROPLASTIC (PTHR47199:SF2)	1039.81	2.72	999.8	2.41
	TraesCS6D02G122800	NADPH-DEPENDENT ALKENAL/ONE OXIDOREDUCTASE, CHLOROPLASTIC (PTHR44573:SF1)	1050.52	1.20	-	-
	TraesCS1B02G308500	PROTEIN MAINTENANCE OF PSII UNDER HIGH LIGHT 1 (PTHR35753:SF2)	918.57	1.36	-	-
	TraesCS1B02G237700	CHLOROPHYLL SYNTHASE, CHLOROPLASTIC (PTHR42723:SF1)	660.6	1.62	662.02	1.42
	TraesCS1B02G237701	CHLOROPHYLL SYNTHASE, CHLOROPLASTIC (PTHR42723:SF1)	661.6	1.63	662.02	1.42
	TraesCS3B02G490600	GLUTATHIONE S-TRANSFERASE F13 (PTHR43900:SF72)	1569.3	1.26	2498.24	1.78
	TraesCS6A02G000300	SKP1-LIKE PROTEIN 1 (PTHR11165:SF92)	1037.75	3.94	832.51	3.88
	TraesCS1D02G454400	HISTONE DEACETYLASE HDT2-like (XP_044452191.1; NCBI)	514.59	5.55	518.65	5.77
	TraesCS2D02G491700	TLD-DOMAIN CONTAINING NUCLEOLAR PROTEIN (PTHR23354:SF104)	523.47	1.17	322.26	1.14
	TraesCS3B02G612000	FLAVONE 3'-O-METHYLTRANSFERASE 1 (PTHR11746:SF199) (CL: Caffeic acid O-methyltransferase?)	1279.95	1.22	-	-

464

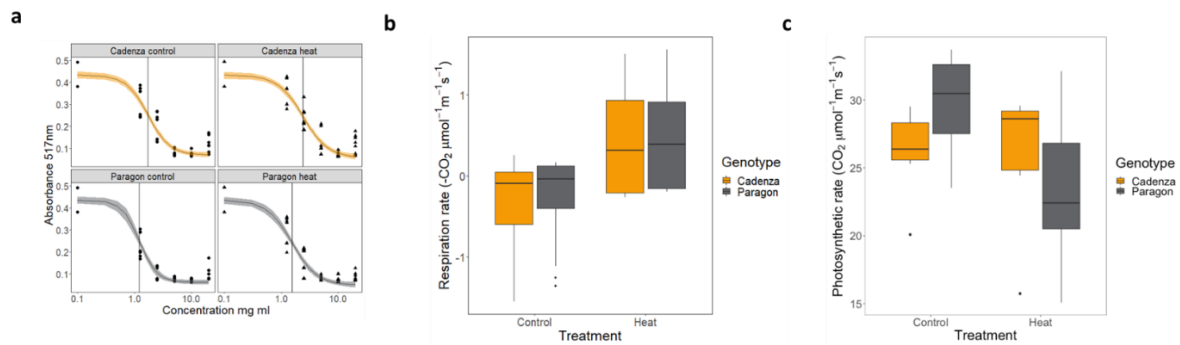
465

466

467 **Chemical ROS scavenging**

468 The capacity for chemical radical scavenging was assessed in control and heat-stressed plants in the
 469 afternoon in two independent experiments with similar results using the standard DPPH assay. Data
 470 of the second experiment, for which an independent set of plants was grown under control and heat
 471 conditions, is shown in Figure 8a. Data are expressed as IC50 values, i.e., the concentration of plant
 472 leaf extract required to reduce the activity of DPPH by 50%. Smaller IC50 values are therefore
 473 indicative of a greater free-radical quenching capacity. The data show overall smaller IC50 values in
 474 Paragon and an increase in IC50 under heat stress in both genotypes, suggesting that the scavenging
 475 capacity under heat is compromised.

476



477

478 **Figure 8. Chemical radical scavenging and photosynthesis under heat stress.**

479 Radical scavenging capacity was measured using the DPPH assay (a) showing a decrease under heat
 480 stress in both genotypes and an overall lower IC50 values in Paragon, indicative of a higher chemical
 481 scavenging capacity. Photosynthetic parameters were measured in Paragon and Cadenza plants
 482 grown under control and heat stress conditions using a Li-Cor Li-6400XT. Respiration rate increased
 483 under heat stress (b) and was overall similar in the two genotypes. The photosynthetic rate was higher
 484 in Paragon under control conditions but significantly lower under heat conditions compared with
 485 Cadenza (c).

486

487

488 Photosynthesis measurement

489 The same plants sampled for the DPPH assay were used for Licor measurements at pre-dawn and PM
 490 using six-week-old plants. There were no significant differences in ΦPSII , $\text{Fv}'\text{Fm}'$, dark respiration, or
 491 stomatal conductance between the two genotypes under heat stress (Figure 8b; data not shown). In
 492 contrast, the photosynthetic rate was significantly lower under heat stress compared with control
 493 conditions, based on a linear regression with photosynthetic rate predicted by genotype and
 494 treatment, (Figure 8c). There was a significant interaction between genotype and treatment, with
 495 Paragon showing a significantly higher photosynthetic rate under control conditions. However, under
 496 heat stress the photosynthetic rate significantly dropped in Paragon whilst Cadenza was able to
 497 maintain its photosynthetic rate in agreement with its suggested heat tolerance (Figure 8c).

498

499

500 Discussion

501 Comparative phenotypic assessment of two spring wheat varieties, Cadenza and Paragon, showed
 502 differences in plant height and tiller number at a T_{max} of 24°C , and a progressive reduction in yield with
 503 increasing temperature. Cadenza was more resilient overall and maintained a higher yield under stress

504 compared to Paragon. This was attributed to excessive tillering and a higher final spike number under
505 high temperatures.

506 Subsequent metabolomic and RNAseq analyses revealed an interesting set of heat-responsive
507 metabolites and genes, as well as significant constitutive genotypic differences.

508

509 **Anti-freeze molecules and other unusual metabolites respond to heat stress in wheat**

510 The metabolites that showed the most significant heat response in both genotypes were three
511 propane-1,2-diol glycosides. The non-glycosylated molecule propane-1,2-diol (or propylene glycol) has
512 a broad range of industrial uses, e.g., as an anti-freeze fluid, as an additive in cosmetics and medicines,
513 as well as being an emulsifier in food, such as ice cream. To our knowledge, this is the first report of
514 propane-1,2-diol in relation to heat stress and only one relevant plant-based study has been
515 published, suggesting that propane-1,2-diol, as a compound in an essential oil product, could promote
516 root growth in lettuce (Nakajima et al., 2005). According to KEGG, propane-1,2-diol is a component of
517 the propanoate metabolism pathway ([map00640](#)) and is synthesized from glycolysis-derived
518 glycerone-P. Industrial uses suggest that it enhances viscosity of fluids and it is interesting to speculate
519 that high levels of propane-1,2-diol in the cytoplasm might reduce heat-induced increase in Brownian
520 motion, or otherwise stabilize cellular compounds and processes. It would be interesting to assess
521 whether propane-1,2-diol levels also increase under cold stress.

522 Also highly increased under heat stress are two DIBOA glycosides and the precursor tryptophane. In
523 contrast, DIMBOA glycoside, the end-product of the benzoxazinoid pathway, which carries an
524 additional methoxy group, was reduced under heat compared to controls. DIBOA has recently been
525 shown to increase under severe drought in bread wheat (Itam et al., 2020). Benzoxazinoids are well
526 known for their role in plant defence against insects, as well as pathogenic microorganisms (Makowska
527 et al., 2015; Zhou et al., 2018) and also affect the microbiome (Cotton et al., 2019). Because
528 benzoxazinoids are potentially autotoxic, activity is controlled via two-component defence systems,
529 i.e., reactivity is reduced by chemical modification, such as glycosylation, whilst simultaneously a
530 reactivating enzyme is provided, e.g., a glycosidase (Niculaes et al., 2018). It has been shown that
531 DIMBOA and DIBOA glycosides are inactive (Hashimoto & Shudot, 1996; Larsen & Christensen, 2000).
532 In Cadenza, DIMBOA glycoside is constitutively higher and, although reduced, remains higher under
533 heat stress compared to Paragon. In agreement with that, a glucosyltransferase gene (*BX8*) was more
534 highly expressed constitutively in Cadenza. On the other hand, two DIMBOA glucosidase genes were
535 significantly increased under heat stress in both genotypes, and three additional genes showed
536 genotype-specific expression. It thus appears that the benzoxazinoid pathway in wheat is heat

537 responsive and finely regulated and it will be interesting to establish its role in abiotic stress tolerance
538 in more detail.

539

540 Another molecule identified in this study, which was significantly higher in Cadenza compared to
541 Paragon and reduced under heat stress, is dhurrin (or dhurrin isomer). Similar to DIBOA/DIMBOA,
542 dhurrin is regulated by a two-component defence system to prevent autotoxicity (Bjarnholt et al.,
543 2018). Dhurrin is a well-known cyanogenic glucoside from sorghum and functions as a chemical
544 defence against herbivores and pathogens by releasing toxic hydrogen cyanide. It is developmentally
545 regulated and can reach toxic levels in young plants, as well as under drought and under highly
546 fertilized conditions (Gleadow et al., 2015; Rosati et al., 2019; Sohail et al., 2022). It has been suggested
547 that cyanogenic glucosides might also serve as an alternative N source and it has recently been shown
548 that dhurrin spontaneously builds conjugates with glutathione, which then undergo reductive
549 cleavage by glutathione transferases, eventually leading to formation of free ammonia by nitrilases
550 (Bjarnholt et al., 2018). Given the high concentration of dhurrin under control conditions in Cadenza,
551 it will be of interest to investigate its function in wheat as a putative alternate N source.

552

553 **Phenolic metabolite profiles suggest an essential role in radical scavenging**

554 Phenylpropanoids and flavonoids are vastly heterogenous groups consisting of thousands of
555 phenylalanine-derived secondary metabolites with important functions throughout plant growth and
556 development, as well as tolerance to biotic and abiotic stresses, including heavy metals, drought,
557 salinity, nutrients, cold and heat (di Ferdinando et al., 2012; A. Sharma et al., 2019) (Dwivedi et al.,
558 2017). The protective function of these molecules is mainly ascribed to their ability to scavenge
559 excessive radicals that form under stress, thereby preventing lipid peroxidation, oxidation of macro-
560 molecules (e.g., DNA, proteins) as well as PSII. However, as is the case for DIBOA and dhurrin,
561 phenylpropanoids can be toxic and it has been shown that glycosylation by UDP-glycosyltransferases
562 reduces toxicity, and modifies solubility, compartmentalization, and stability, whilst reducing
563 antioxidant capacity (le Roy et al., 2016; Shahidi et al., 2022). Likewise, multiple methoxy-groups on
564 one phenolic ring might reduce reactivity and antioxidant capacity and are thus important regulatory
565 functional groups (Jeevitha et al., 2017; Teponno et al., 2016).

566 Tri-methoxy cinnamic acid was the most significantly increased metabolite of the phenylpropanoid
567 pathway under heat stress, in both Cadenza and Paragon. Cinnamic acid is the first product of the
568 general phenylpropanoid pathway catalyzed by the enzyme PAL (phenylalanine ammonium lyase) and
569 the precursor for derived ferulic and coumaric acid. The role of the three methoxy groups is not
570 entirely clear. As was shown in an animal study, tri-methoxy cinnamic acid had a strong protective role

571 against gastric lesions (Lee et al., 2017), however, anti-cancer properties and DPPH radical scavenging
572 properties were dependent on the nature of functional groups and the number of methoxy groups, as
573 already mentioned above (Ruwizhi & Aderibigbe, 2020; Takahashi & Kakehi, 2010). Although ferulic
574 acid was reduced under heat, it remained significantly higher in Cadenza, compared to Paragon, due
575 to the high concentration under control conditions. Ferulic acid is, in its covalently conjugated form
576 an important component of cell walls, whilst it acts as an antioxidant and anti-cancer compound in its
577 free form (N. Kumar & Pruthi, 2014). Likewise, syringic acid derivatives remained higher in Cadenza
578 despite being reduced under heat. Syringic acid has a wide range of health benefits including free-
579 radical scavenging which has been attributed to the methoxy groups on the aromatic ring at positions
580 3 and 5 (Srinivasulu et al., 2018). Constitutive genotypic differences have also been reported from a
581 study on drought, showing constitutively higher levels of chlorogenic acid, ferulic acid and other
582 shikimate-derived metabolites in the intolerant genotype and general reduction under stress (Guo et
583 al., 2018).

584 Contrary to free ferulic acid, feruloyl-coumaroyl-glycerol conjugates increased under heat in both
585 genotypes to about the same level. Radical scavenging and antioxidant activity of the conjugate has
586 been shown in extracts of *Tulipa systole*, a herbal medicine from Iraq (Ibrahim et al., 2017). An increase
587 in this conjugate might therefore provide effective protection against ROS damage. This is in support
588 of a study in rice, which identified 4-hydroxycinnamic acid and ferulic acid as key metabolites related
589 to the higher level of drought tolerance in a tolerant genotype (IAC1246), which also maintained a
590 higher level of photosynthesis and antioxidant capacity (X. Ma et al., 2016). An increase in caffeic acid
591 and ferulic acid has also been reported from a study in festuca and this was specific to the tolerant
592 genotype in response to a short term (7h) but not long-term (21h) heat stress (J. Wang et al., 2019).
593 Similarly, differences in metabolic responses to cyclic versus prolonged drought stress has been shown
594 in poplar, with the former mainly affecting primary metabolites, whereas the latter induced mainly
595 secondary metabolites (populosides) (Tschaplinski et al., 2019), which is in agreement with the
596 response to chronic heat stress reported here.

597 In a detailed study in tomato, plants were exposed to heat and salt stress and a combination of the
598 two stresses (Martinez et al., 2016). The study showed a differential accumulation of
599 phenylpropanoids and flavonoids, with the latter specifically increased under heat stress and
600 associated with greater protection from oxidative damage. Flavonoids are known to be powerful
601 antioxidants, especially dihydroxy-B-ring substituted flavonoids, such as caffeic acid, tricetin or
602 luteolin, (Agati et al., 2012). It was shown in maize, that higher drought tolerance in a mutant (*doi*)
603 was related to higher total flavonoid content and ROS scavenging capacity compared to the B73
604 wildtype control (Li et al., 2021). Constitutive genotypic difference in flavonoids have also been shown

605 in Arabidopsis and rice (C. Hu et al., 2014; Routaboul et al., 2012) and the role of flavonoids as
606 antioxidants under drought stress have been shown in wheat (D. Ma et al., 2014) as well as by
607 transgenic approaches in Arabidopsis (Nakabayashi et al., 2014; Rao et al., 2020) and apple (Geng et
608 al., 2020).

609 In our study, we found a large increase of an unspecified, glycosylated flavonoid compound that was
610 highly significantly upregulated under heat stress. Interestingly, whilst three derivatives of this
611 compound were increased in both analyzed genotypes, other derivatives were highly specific to
612 Cadenza and Paragon, respectively. Other compounds that increased under heat stress included
613 molecules derived from tricin, tricitin and chryseriol. As was the case for the phenylpropanoids, some
614 flavonoid compounds were reduced under heat stress but showed constitutive genotypic differences
615 with an apparent overall higher abundance in Cadenza.

616 However, despite these marked genotypic differences, DPPH assay data from two independent
617 experiments revealed an overall slightly higher ROS scavenging capacity in Paragon, as indicated by a
618 lower IC50 value. This suggests that chemical radical scavenging is well developed in both genotypes
619 and that tolerance in Cadenza might thus be related to other mechanisms.

620

621 **Differential expression of stress-response genes**

622 The RNAseq analysis revealed a range of genes with known protective functions under stress. In
623 Cadenza, candidate genes encode a peroxidase and an aldehyde dehydrogenase, which detoxify
624 aldehydes originating from lipid hydroperoxides (Kotchoni et al., 2006; Sunkar et al., 2003). In addition,
625 a large number of glutathione S-transferases (GSTs) were upregulated in both genotypes. GSTs
626 detoxify electrophilic compounds by catalyzing the nucleophilic conjugation of GSH (γ -Glu-Cys-Gly)
627 and have been implicated in many stress responses (Jain et al., 2010; Nutricati et al., 2006; Sappl et
628 al., 2009; R. Sharma et al., 2014; Skopelitou et al., 2017). Surprisingly, thioredoxins, which also have
629 been implicated with a range of protective functions under stress (Delaunay et al., 2002; Zhai et al.,
630 2022) were downregulated under heat stress in both genotypes.

631 Cell membranes are particularly sensitive to high temperature stress because increased kinetic energy
632 loosens chemical bonds leading to increased fluidity, and therefore permeability (Niu & Xiang, 2018).
633 Membranes are also sensitive to ROS and lipid peroxidation is a key indicator of heat stress (Jiang &
634 Huang, 2001). As a result of these effects, electrolytes can be lost, and the membrane is unable to
635 perform its required function, which can ultimately lead to cell death (Narayanan et al., 2015, 2018;
636 Narayanan, Prasad, et al., 2016; Narayanan, Tamura, et al., 2016). Our RNAseq analysis revealed
637 differential expression and positive heat-response in Cadenza of several genes encoding lipid-related
638 proteins, including a lipase GDSL domain-containing protein and a non-specific lipid-transfer protein

639 (nsLTP) 2G. Both GELPs and nsLTPs play crucial roles in plant growth and development (R. Ma et al.,
640 2018; Watkins et al., 2019), and have demonstrated roles in biotic and abiotic stresses (H. G. Kim et
641 al., 2013; Naranjo et al., 2006). There is evidence that both GELPs and nsLTPs play a role in male
642 reproductive development (M. der Huang et al., 2013; Wan et al., 2020; J. Zhao et al., 2020a).
643 Interestingly, *nsLTPs* also have a role in protecting thylakoid membranes during freezing (Hincha et al.,
644 2001, 2002; Srór et al., 2003). This and the above-mentioned identification of the anti-freeze propane-
645 diol suggests communalities between heat and cold stress responses.

646 Another major problem under heat stress is the degradation of proteins and, as a protective measure,
647 plants upregulate HSPs to facilitate re-folding and re-solubilisation of denatured proteins and protein
648 aggregates (Bourgine & Guihur, 2021; A. Kumar et al., 2020a). In the RNAseq study, six HSP70 genes
649 were identified, with a general trend towards downregulation in Cadenza and upregulation in
650 Paragon. However, two of these genes showed constitutively lower expression in Paragon, despite the
651 heat-induced upregulation. One of these encodes *BINDING IMMUNOGLOBULIN PROTEIN* (BiP), one of
652 the major chaperones in the ER lumen (Pobre et al., 2019). In the ER, heat stress induces the so-called
653 Unfolded Protein Response (UPR) (Angelos et al., 2017; Buchberger et al., 2010; Liu & Howell, 2010;
654 Read & Schröder, 2021) which is a protective pathway increasing the ER's protein folding capacity.
655 BiP-encoding genes have been shown to be upregulated by the UPR and play a protective role during
656 drought and osmotic stress (Alvim et al., 2001; Carvalho et al., 2014; Valente et al., 2009), possibly by
657 preventing endogenous oxidative stress (Alvim et al., 2001). Constitutively higher expression of this
658 gene in Cadenza could contribute to the observed tolerance to heat stress in this study.

659 HSP70s work in conjunction with small Heat Shock Proteins (sHSP) to protect their thermo-sensitive
660 substrates (Bourgine & Guihur, 2021; Waters & Vierling, 2020). Expression of a sHSP was consistently
661 higher in Cadenza but increased in Paragon under HT. The stress-responsive and protective functions
662 of these chaperones may contribute to the heat tolerance seen in Cadenza. Two HSP80s and four
663 HSP100 genes were also upregulated in both cultivars under heat, as were several peptidylprolyl
664 isomerase, which are known to interact with HSPs to regulate protein biosynthesis and refolding of
665 proline-containing proteins (Kaur et al., 2015; Kurek et al., 1999). Peptidylprolyl isomerases,
666 specifically AtFKBP6/ROF1, are also part of a well-studied heat response in which FKBP interacts with
667 HSP90 and, in a heat-dependent manner, with the heat shock transcription factor HSFA2A. Nuclear
668 translocation of this complex then enables the HSFA2A-dependent transcription of sHSP genes (Meiri
669 & Breiman, 2009). An FKBP gene has previously also been identified as a candidate in a study on heat
670 tolerance in rice (González-Schain et al., 2016).

671 Another important chaperone family are dehydrins, which are shown to stabilize membranes
672 (Eriksson et al., 2016) and prevent protein aggregation and/or inactivation under stress (Close, 1997;

673 Park et al., 2006; Qin & Qin, 2016; Yu et al., 2018). Dehydrins also act as radical-scavengers due to
674 their high content of histidine, lysine and glycine, which are targets for radical-mediated oxidation
675 (Drira et al., 2013; Hara et al., 2004, 2005; W. Yang et al., 2015). Two dehydrin genes, annotated as
676 *RAB15* and *RAB16B*, showed increased expression under heat in Cadenza, and the dehydrin gene
677 *CS120* remained stable in Cadenza whilst decreasing under HEAT in Paragon. *CS120* has been
678 implicated in membrane protection during drought and cold stress (Chu et al., 2021).

679 Taken together, the nature of the identified DEGs suggest that Cadenza might have a greater capacity
680 to prevent protein degradation, membrane damage and the ER UPR response.

681 Several other genes involved in effective protein synthesis, processing, ubiquitination and degradation
682 were amongst the differentially expressed genes. These include an F-box domain containing protein,
683 an aldo_ket_red domain-containing protein, and an AA-trans domain containing protein. This suggests
684 a different response or capacity for coping with protein mis-folding. A cysteine protease, known to be
685 responsive to environmental cues (Morrell & Sadanandom, 2019) and play a part in oxidative stress-
686 induced programmed cell death (Solomon et al., 1999) showed constitutively higher expression in
687 Cadenza. Also higher in Cadenza were ankyrin repeat (ANK) genes which have essential roles in plant
688 development and have been shown to respond to heat and cold stress (Eun et al., 2007; X. Yang et al.,
689 2008). Overexpression of *ANK genes* have been shown to mitigate the effects of drought (X. Yang et
690 al., 2008) and oxidative stress (Seong et al., 2007) in *Artemesia desertorum* and Capsicum,
691 respectively. Despite evidence of the role of members of this protein family in response to stress, their
692 roles in heat stress have not been well characterised, with no information available for their activity
693 in wheat. The genes highlighted in this study have not previously been linked to heat stress, so would
694 therefore be novel targets for further investigation into heat stress tolerance in wheat.

695 Other relevant genes include xyloglucan endotransglucosylase/hydrolase (XTHs) and Polysaccharide
696 synthesis 4 (PS4) domain-containing protein, both involved in cell wall biogenesis and remodelling.
697 XTHs correlate with plant growth (Osato et al., 2006; van Sandt et al., 2007; Vissenberg, Fry, et al.,
698 2005; Vissenberg, Oyama, et al., 2005) and decrease in expression in response to heat, as observed in
699 Paragon, has also been shown in other wheat cultivars (Iurlaro et al., 2016). Maintenance of
700 expression of these genes under stress in Cadenza might thus be a factor contributing to its superior
701 growth and tillering capacity under stress.

702 Two hormone-related genes, *ABSCISIC STRESS-RIPENING PROTEIN 5 (ASR5)* and *CYTOKININ*
703 *DEHYDROGENASE 3*, showed higher expression in Cadenza. ASR proteins have been implicated in a
704 range of stresses, including heat and cold, and they enhance drought tolerance in Arabidopsis by
705 upregulating ABA/stress-regulated genes and acting as chaperone-like proteins (Golan et al., 2014;
706 Sah et al., 2016; Yacoubi et al., 2022). Interestingly, one of the heat-induced genes in Cadenza codes

707 for a fructan exohydrolase (FEH). Fructans function as both short-term storage polysaccharides and in
708 stabilising membranes during freezing and drought, acting as signalling molecules, and exerting an
709 antioxidant effect (van den Ende, 2013).

710

711 **Cadenza maintains photosynthesis under heat stress**

712 One of the key findings of this study was that Cadenza maintained photosynthetic rate under heat
713 stress whilst it was significantly reduced in Paragon. Thylakoid membranes, electron carriers and
714 enzymes, particularly those of PSII are thermosensitive (Moore et al., 2021; Salvucci & Crafts-
715 Brandner, 2004a; Sharkey, 2005). High temperatures lead to an excess of chloroplastic reducing
716 equivalent, accumulation of ROS and photoinhibition (S. Hu et al., 2020b; X. Wang et al., 2017). The
717 above-described differences in the chemical and non-chemical radical scavenging capacity between
718 the genotypes might therefore be an important factor protecting PSII.

719 Of the photosynthesis-related heat-responsive DEGs, a similar expression was observed in Cadenza
720 and Paragon. Whilst the majority of these genes was downregulated under heat, the three homeologs
721 of RuBisCo activase were all upregulated under heat stress. Rubisco activase is essential for the
722 maintenance of the carboxylation reaction but is particularly sensitive to heat (Law & Crafts-Brandner,
723 1999; Ristic et al., 2009; Salvucci & Crafts-Brandner, 2004b). Interestingly, it has recently been shown
724 *in vitro* that a single amino acid substitution increased thermotolerance and activity under heat (Degen
725 et al., 2020b). It has also been shown that overexpression of both Rubisco and Rubisco activase
726 increases photosynthesis under heat stress in rice (Qu et al., 2021)

727 This does not explain the observed genotypic differences in photosynthetic thermotolerance, which
728 could instead be related to the photosynthesis-associated genes that showed constitutively different
729 expression. Of particular interest in this context are genes with higher expression in Cadenza, encoding
730 e.g., a PsbP domain-containing protein, PROTEIN LOW PSII ACCUMULATION 3 (LPA3), and an
731 unspecified Rieske domain-containing protein. PsbP-like proteins are involved in the assembly of PSII
732 and it was shown in Arabidopsis that PsbPs optimize the water-oxidizing reaction and are required for
733 the efficient repair of photodamaged PSII (Che et al., 2020). Likewise, LPA3 has been implicated in PSII
734 repair (Theis & Schroda, 2016). Rieske proteins are Fe-S proteins, and as a subunit of Cytb6f, an
735 essential component of PSII electron transport. Overexpression of the Brachipodium PetC gene in
736 Setaria has recently been shown to enhance C4 photosynthesis (Ermakova et al., 2019).

737

738 **Conclusions**

739 This study reveals genotypic differences in vegetative heat tolerance within UK spring wheat and
740 highlights the importance of secondary metabolites for stress resilience, due to their protective role

741 via chemical radical scavenging. The identification of propane-diol as a novel, highly heat-induced
742 compound warrants further investigation and suggests communalities between heat and cold
743 responses. The gene expression data confirmed the general role of heat-induced chaperones and ROS
744 scavenging pathways and further suggests that constitutive genotypic differences might be important
745 for stress tolerance. Maintenance of photosynthesis in Cadenza under heat has been identified as a
746 key component of tolerance and future work will establish whether this is related to the differentially
747 expressed photosynthesis-related genes or any other Cadenza-specific heat-responsive genes with
748 putative protective functions.

749

750 **Materials and Methods**

751 **Plant material and growth conditions:**

752 Two UK spring wheat varieties, Cadenza and Paragon, were used in this study. Seeds were surface
753 sterilised and pre-germinated seeds transplanted into fully fertilized potting mix as described by
754 (Oszvald et al., 2022).

755 **Pilot study:** Plants were grown in a controlled environment glasshouse at 20°C with 16 h light for one
756 week before transfer into Sanyo Gallenkamp growth cabinets (70% relative humidity, 13.5 h light,
757 fluorescent light 400 $\mu\text{mol m}^{-2} \text{s}^{-1}$). Lights and temperatures were ramped up over a period 30 min.
758 Plants were grown in a randomized complete block design with four replications under five different
759 maximum day temperatures (T_{max}) and corresponding 6°C cooler night temperatures: 18°C/12°C,
760 21°C/15°C, 24°C/18°C, 27°C/21°C and 30°C/24°C day/night. T_{max} was maintained for 12h. At the end
761 of the flowering stage, plants were returned to the glasshouse and supplemental lighting of 250 μmol
762 $\text{m}^{-2} \text{s}^{-1}$ was provided as required until harvest. Plants were kept well-watered at all times.

763 To assess the effect of T_{max} , plant height (PH; longest leaf) and tiller number (TN) were recorded at
764 seven time-points until 50 days after germination. At harvest, the final plant height (tip of awnless
765 spike) and final tiller and spike number were recorded. Above-ground material was oven-dried at 80°C
766 for 16h to determine straw dry weight (DW). Spikes were threshed by hand to determine total seed
767 weight, as well as other detailed seed parameters (see main text) using a MARViN seed analyser for
768 small seeds (MARViTECH GmbH Germany). Grain hardness, individual seed weight, moisture and
769 diameter were determined using the Perten Single Kernel Characterisation System (SKCS) 4100
770 following the manufacturer's procedure. One hundred grains for each plant from each replicate were
771 used for each analysis (Perten Instruments, Calibre Control International Ltd, UK).

772

773 **Sampling for RNAseq and metabolomics analyses, and physiological measurements**

774 For isolation of RNA and metabolites Cadenza and Paragon plants were grown at 21°C/15°C and
775 27°C/21°C as described above. An independent set of plants were grown under the same conditions
776 for measurements of photosynthesis and enzyme activities (see below).

777 Samples for RNAseq and metabolomics analyses were collected pre-dawn and in the afternoon (PM)
778 after plants were exposed to T_{max} for 5-6 h. Plants were removed from the cabinets individually and
779 immediately processed. Samples were taken at three timepoints, over a period of 47 days,
780 corresponding to 26d (TP1), 39d (TP2), and 47d (TP3) days after germination. Individual plants were
781 sampled, with four replicates for each treatment and genotype. At TP1 the entire seedling (4-5 leaf
782 stage) was harvested, at TP2 the main tiller was harvested, and at TP3 the youngest fully expanded
783 leaf of the main tiller was harvested. This corresponds to a total of 96 samples, i.e., 48 samples for
784 each, Cadenza and Paragon. The fresh weight (FW) was recorded and the material was immediately
785 frozen in liquid nitrogen and stored at -80°C until further use.

786

787 **RNAseq analysis**

788 For RNA extraction, the 96 samples were hand ground in liquid nitrogen and RNA was extracted from
789 100mg aliquots using TRIzol™ according to the manufacturer's protocol (Invitrogen, UK). The RNA
790 samples were analyzed by Novogene (HK) Company Limited (Hong Kong) using an Illumina PE 150
791 (Q30 ≥80%) and was based on a Eukaryotic RNA-seq (library preparation and sequencing with 250-300
792 bp inserts) according to the company's specifications (March 2019). The quality of the obtained raw
793 sequences was assessed with FastQC (<http://www.bioinformatics.babraham.ac.uk/projects/fastqc/>
794 (2015), "FastQC," <https://qubeshub.org/resources/fastqc.>) with a mean Q30(%) = 94% and mean clean
795 read ratio of 97.83%. Based on this, six samples were excluded from further analysis. The overall
796 alignment rate for all samples was 91.3% using the HISAT2 aligner (D. Kim et al., 2015). The data are
797 available at the European Nucleotide Archive (ENA) under accession number PRJEB36237 and unique
798 name ena-STUDY-ROTHAMSTED RESEARCH-15-01-2020-14:13:41:981-1984.

799

800 **Nuclear magnetic resonance spectroscopy (NMR)**

801 An aliquot of the ground tissue samples used for RNA extraction was subjected to primary and
802 secondary metabolomic analysis, by NMR and LCMS respectively, at the Rothamsted Research
803 metabolomics facility. For NMR, 1H-NMR samples were prepared from milled, freeze-dried leaf
804 samples (15 mg) extracted in triplicate using 80:20 D2O:CD3OD containing 0.01% d4-
805 trimethylsilylpropionate (TSP) (1ml) as internal standard. After agitation, samples were extracted at
806 50 °C for 10 minutes. After centrifugation (5 minutes at 13,000 rpm), the supernatant was removed
807 to a clean tube and heated to 90°C for 2 minutes to halt enzyme activity. After cooling and further

808 centrifugation, the supernatant (650 μ L) was transferred to a 5mm NMR tube for analysis. ^1H -NMR
809 spectra were acquired under automation at 300°K using an Avance Spectrometer (BrukerBiospin,
810 Coventry, UK) operating at 600.0528 MHz and equipped with a cryoplatfrom and a 5 mm triple inverse
811 cryoprobe. Spectra were collected using a water suppression pulse sequence with a 90° pulse and a
812 relaxation delay of 5 s. Each spectrum was acquired using 128 scans of 64,000 data points with a
813 spectral width of 7309.99 Hz. Spectra were automatically Fourier-transformed using an exponential
814 window with a line broadening value of 0.5 Hz. Phasing and baseline correction were carried out within
815 the instrument software. ^1H chemical shifts were referenced to d4-TSP at δ 0.00. ^1H -NMR spectra
816 were automatically reduced, using Amix (Analysis of MIXtures software, BrukerBiospin), to ASCII files
817 containing integrated regions or 'buckets' of 0.01 ppm equal width. Spectral intensities were scaled
818 to the d4-TSP region (δ 0.05 to $-$ 0.05). The ASCII file was imported into Microsoft Excel for the addition
819 of sampling/treatment details. Signal intensities for characteristic spectral regions were extracted via
820 comparison to library spectra of known standards run under identical conditions. Quantitation against
821 a known concentration of d4-TSP was carried out using the known number of hydrogens responsible
822 for each characteristic peak of each metabolite.

823

824 **Liquid chromatography–mass spectrometry (LC–MS)**

825 Leaf samples were prepared as described for NMR, except that the extraction solvent was 80:20
826 H_2O :MeOH. UHPLC–MS were recorded with an Dionex UltiMate 3000 RS UHPLC system, equipped
827 with a DAD-3000 photodiode array detector, coupled to an LTQ-Orbitrap Elite mass spectrometer
828 (Thermo Fisher Scientific, Germany). UHPLC separation was carried out using a reversed-phase
829 Hypersil GOLD™ column (1.9 μ m, 30 \times 2.1 mm i.d. Thermo Fisher Scientific, Germany) which was
830 maintained at 35°C. The solvent system consisted of water/0.1% formic acid (A) and acetonitrile/0.1%
831 formic acid (B), both Optima™ grade (Thermo Fisher Scientific, Germany). Separation was carried out
832 for 40 min under the following conditions: 0-5 min, 0% B; 5-27 min, 31.6% B; 27-34 min, 45% B; 34-
833 37.5 min, 75% B. The flow rate was 0.3 mL/min, and the injection volume was 10 μ L. Mass spectra
834 were collected in negative ion mode using an LTQ-Orbitrap Elite with a heated ESI source (Thermo
835 Fisher Scientific, Germany). Spectra were acquired with a resolution of 120,000 over m/z 50–1500.
836 The source voltage, sheath gas, auxiliary gas, sweep gas and capillary temperature were set to 2.5 kV,
837 35 (arbitrary units), 10 (arbitrary units), 0.0 (arbitrary units) and 350°C, respectively. Default values
838 were used for other acquisition parameters. Automatic MS–MS was performed on the four most
839 abundant ions and an isolation width of m/z 2 was used. Ions were fragmented using high-energy C-
840 trap dissociation with a normalised collision energy of 65 and an activation time of 0.1 ms. Data were
841 inspected using Xcalibur v. 2.2 (Thermo Fisher Scientific, Germany). For comparison between samples,

842 spectra were processed in Compound Discoverer software using the “Untargeted Metabolomics
843 Workflow”. Annotations were made by comparison to known standards run under the same
844 conditions where possible. Putative identifications were made via comparison to literature of known
845 wheat metabolites via the use of Reaxys databases (<https://library.udel.edu/databases/reaxys/>).

846

847 **Photosynthesis measurements**

848 Gas exchange and leaf fluorescence were measured using LI-6400XT portable photosynthesis systems
849 (Li-Cor Inc., USA) equipped with leaf chamber fluorometers (LI-6400XT, Li-Cor Inc., 1 USA).
850 Measurements were taken from plants grown under heat (27°C/21°C) and control (21°C/15°C)
851 conditions, as described above, at six weeks after transplanting, and again four days later.

852 Measurements were taken during a two-hour pre-dawn period and a two-hour period in the
853 afternoon, after plants were exposed to maximum light intensity and temperature for about six hours.

854 A total of sixteen plants (four plants of each genotype and treatment) were measured in parallel, using
855 two LI-6400XT systems alternately for half of the plants according to the blocks of the randomised
856 design. Respiration, stomatal conductance, and quantum efficiency of photosystem II (Fv/Fm) were
857 measured during the dark period with an air flow of 200 $\mu\text{mol s}^{-1}$, reference CO₂ 400 $\mu\text{mol mol}^{-1}$, block
858 temperature was 15°C for plants from the control cabinet and 21°C for plants from the heat cabinet,
859 photosynthetic active radiation (PAR) of 0 $\mu\text{mol m}^{-2} \text{s}^{-1}$. Photosynthesis and stomatal conductance
860 were measured during the light period with an air flow of 200 $\mu\text{mol s}^{-1}$, reference CO₂ 400 $\mu\text{mol mol}^{-1}$,
861 block temperature was 21°C for plants from the control cabinet and 27°C for plants from the heat
862 cabinet, photosynthetic active radiation (PAR) of 1800 $\mu\text{mol m}^{-2} \text{s}^{-1}$. Relative humidity in the leaf
863 chamber fluorometers was maintained between 50% and 70% throughout all measurements.

864

865 **DPPH assay**

866 Cellular radical scavenging capacity using the DPPH (2,2-diphenyl-1-picrylhydrazyl) method was
867 determined for the same freeze-dried samples (TP1 and TP2) used for the metabolomics analysis.
868 Additional samples were collected from the plants grown for the photosynthesis measurements. For
869 this, the youngest fully extended leaf was harvested from two tillers of four plants per genotype, per
870 heat treatment during peak light intensity and temperature in the sixth hour of the day. Samples (n =
871 16) were flash frozen in liquid nitrogen and stored at -80°C before grinding and freeze-drying for 24h.
872 The assay was conducted using 0.1 mL of 0.03 mM DPPH (Sigma Aldrich, UK) added to 0.1 mL extract
873 at different concentrations (1.25-20 mg of plant tissue/mL). After 30 min of incubation in the dark at
874 room temperature, the absorbance at 517 nm was measured with a spectrophotometer. The
875 antioxidant activity of the extracts is expressed as IC₅₀, which is the concentration (in mg/mL) of

876 extract that inhibits the formation of DPPH radicals by 50%. This was calculated from a four-parameter
877 log-logistic curve fitted in R (version 3.6.1) using the “drc” package.

878

879

880

881 **Statistical analysis**

882 **Phenotypic data**

883 For the phenotypic data derived from the pilot study, a non-linear 3 parameter exponential model
884 was fitted to the plant height (PH) $y = a + (y_0 - a)exp(-rt)$, where y is the response variable, t is
885 the time and y_0, a, r are the model parameters. Only the exponential growth parameter (r) was taken
886 forward for downstream analysis. Data included the final PH at harvest (day 191). For the tiller number
887 (TN) an alternative parameterisation was used $y = a + b exp(rt)$. A high correlation is observed
888 between the linear coefficient and exponential rate, thus in what the gradient of growth at time 0 (\tilde{r}
889 = $r \times b$) is included in the downstream analysis. Non-linear modelling was done in R version 3.6.1 using
890 non-linear least squares. The self-starting asymptotic regression function was used for the plant height
891 model. For multivariate analysis of harvest variables, partial least squares discriminant analysis (PLS-
892 DA) was applied to the set of vegetative traits and harvest variables, with a one-way treatment
893 structure consisting of all cultivar x treatment combinations. Variables were scaled to have unit
894 variance before analysis. PLSDA was done in R version 3.6.1 using the mixOmics package (Rohart et
895 al., 2017)

896

897 **Metabolomics data statistical analyses**

898 The identified differential primary and secondary metabolites (see above) were analysed by univariate
899 analysis using Genstat 20th edition (VSN International Ltd, Hemel Hempstead, UK) using a nested
900 treatment structure whereby a two-way factorial structure investigating line and temperature effects
901 was extracted separately for each sampling occasion:

902 (sampling_time-of-day * sampling TP) /
903 genotypeTP1predawn*tempTP1predawn + genotypeT1pm*tempT1pm +
904 genotypeTP2predawn*tempTP2predawn + genotypeTP2pm*tempTP2pm +
905 genotypeTP3predawn*tempTP3predawn + genotypeTP3pm*tempTP3pm)

906 To establish quantitative differences of metabolites between Cadenza and Paragon, the following
907 nested treatment structure was used whereby a two-way factorial structure investigating line and
908 temporal effects was extracted separately for each temperature by time of day combination:

909 sampling_time-of-day * temperature) /
910 (genotype21Cpredawn*time21Cpredawn + genotype21Cpm*time21Cpm +

911 genotype27Cpredawn *time27Cpredawn + genotype27Cpm*time27Cpm)
912 Analyses were done by fitting a linear mixed model using REML. Random effects included a term
913 accounting for the cabinet.block. Significance of individual treatment terms was done using the
914 Kenward & Roger (1997) approximate F-tests. Multiplicity corrections for the overall false discovery
915 rate were done by applying a Benjamini-Hochberg correction to the one-way test and applying this
916 correction to the set of independent tests for each metabolite according to the rank, filter, model
917 approach of Hassall & Mead (2018). This process was done independently for the NMR and LC-MS
918 data. The Heatmap was constructed in R version 4.0.3 and show the scaled (mean centred and divided
919 by the standard deviation) of the log₂ abundance of all metabolites. Metabolites have been ordered
920 according to a hierarchical clustering with complete linkage of the scaled Euclidean distance.

921

922 **RNAseq data statistical analysis**

923 Based on a PCA analysis, sixteen outliers were identified and removed from further analysis. The
924 remaining eighty samples showed a clear separation between cultivars and sampling time (pre-dawn
925 AM vs PM) and a small separation between growth temperatures. The BioConductor R package
926 DESeq2 was used to fit a generalised linear model to transcript abundances. This accounts for both
927 the design of the experiment and the statistical distribution of the counts, and uses replicates to
928 calculate a fitted value for each gene. Only genes in which eight or more samples (averaged over
929 replicates) had mean raw counts greater than 7 were retained. This gave a counts table for 72,490
930 genes. The following factorial model was applied to the experiment: Cultivar (P, C) x Temperature
931 (T21, T27) x Time (am, pm) x Development stage (ds1, ds2, ds3). DESeq2 was used to fit the full model
932 to the data and extract twenty-four fitted values for each gene.

933

934

935 **AUTHOR CONTRIBUTIONS**

936 All authors contributed to the article and approved the submitted version. SH was leading the project.
937 MW conducted the phenotypic analysis and sampling for molecular analysis. TR conducted the
938 RNAseq experiment. CL conducted the photosynthesis and DPPH measurements. JW and CND
939 conducted the metabolite analyses. KH and DH carried out the statistical analysis of the metabolite
940 and RNAseq data, with inputs from SA, JX, and CL. SH and TR wrote the manuscript, with contributions
941 from JW, KH, and CL.

942

943 **FUNDING**

944 This project was supported by the RCUK project BB/P027970/1 "Transforming India's Green
945 Revolution by Research and Empowerment for Sustainable food Supplies (TIGR2ESS) and the

946 “Designing Future Wheat” (DFW) Strategic Programme. Further support was provided from the UKRI
947 project “Safeguarding Sonora’s wheat from climate change” (BB/S012885/1). SH is also supported by
948 the National Institute of Agricultural Botany (NIAB), Cambridge, UK.

949

950 **ACKNOWLEDGMENTS**

951 We would like to thank the Rothamsted Research greenhouse team for their help with growing the
952 plants. Many thanks to Dan Smith for his support with the RNAseq data analysis.

953

954

955

956 **References:**

957

958 Agati, G., Azzarello, E., Pollastri, S., & Tattini, M. (2012). Flavonoids as antioxidants in plants:
959 Location and functional significance. In *Plant Science* (Vol. 196, pp. 67–76).
960 <https://doi.org/10.1016/j.plantsci.2012.07.014>

961 Alvim, F. C., Carolino, S. M. B., Cascardo, J. C. M., Nunes, C. C., Martinez, C. A., Otoni, W. C., & Fontes,
962 E. P. B. (2001). Enhanced Accumulation of BiP in Transgenic Plants Confers Tolerance to Water
963 Stress. *Plant Physiology*, *126*(3), 1042. <https://doi.org/10.1104/PP.126.3.1042>

964 Angelos, E., Ruberti, C., Kim, S. J., & Brandizzi, F. (2017). Maintaining the factory: the roles of the
965 unfolded protein response in cellular homeostasis in plants. *Plant Journal*, *90*(4), 671–682.
966 <https://doi.org/10.1111/TPJ.13449>

967 Bjarnholt, N., Neilson, E. H. J., Crocoll, C., Jørgensen, K., Motawia, M. S., Olsen, C. E., Dixon, D. P.,
968 Edwards, R., & Møller, B. L. (2018). Glutathione transferases catalyze recycling of auto-toxic
969 cyanogenic glucosides in sorghum. *Plant Journal*, *94*(6), 1109–1125.
970 <https://doi.org/10.1111/tpj.13923>

971 Bourguin, B., & Guihur, A. (2021). Heat Shock Signaling in Land Plants: From Plasma Membrane
972 Sensing to the Transcription of Small Heat Shock Proteins. *Frontiers in Plant Science*, *12*, 1583.
973 <https://doi.org/10.3389/FPLS.2021.710801/BIBTEX>

974 Buchberger, A., Bukau, B., & Sommer, T. (2010). Protein Quality Control in the Cytosol and the
975 Endoplasmic Reticulum: Brothers in Arms. *Molecular Cell*, *40*(2), 238–252.
976 <https://doi.org/10.1016/J.MOLCEL.2010.10.001>

977 Carvalho, H. H., Brustolini, O. J. B., Pimenta, M. R., Mendes, G. C., Gouveia, B. C., Silva, P. A., Silva, J.
978 C. F., Mota, C. S., Soares-Ramos, J. R. L., & Fontes, E. P. B. (2014). The Molecular Chaperone
979 Binding Protein BiP Prevents Leaf Dehydration-Induced Cellular Homeostasis Disruption. *PLOS*
980 *ONE*, *9*(1), e86661. <https://doi.org/10.1371/JOURNAL.PONE.0086661>

981 Che, Y., Kusama, S., Matsui, S., Suorsa, M., Nakano, T., Aro, E. M., & Ifuku, K. (2020). Arabidopsis
982 PsbP-Like Protein 1 Facilitates the Assembly of the Photosystem II Supercomplexes and

- 983 Optimizes Plant Fitness under Fluctuating Light. *Plant and Cell Physiology*, 61(6), 1168–1180.
984 <https://doi.org/10.1093/pcp/pcaa045>
- 985 Cheabu, S., Moug-Ngam, P., Arikkit, S., Vanavichit, A., & Malumpong, C. (2018). Effects of Heat Stress
986 at Vegetative and Reproductive Stages on Spikelet Fertility. *Rice Science*, 25(4), 218–226.
987 <https://doi.org/10.1016/j.rsci.2018.06.005>
- 988 Chu, C., Wang, S., Paetzold, L., Wang, Z., Hui, K., Rudd, J. C., Xue, Q., Ibrahim, A. M. H., Metz, R.,
989 Johnson, C. D., Rush, C. M., & Liu, S. (2021). RNA-seq analysis reveals different drought
990 tolerance mechanisms in two broadly adapted wheat cultivars “TAM 111” and “TAM 112.”
991 *Scientific Reports*, 11(1). <https://doi.org/10.1038/S41598-021-83372-0>
- 992 Close, T. J. (1997). Dehydrins: A commonality in the response of plants to dehydration and low
993 temperature. *Physiologia Plantarum*, 100(2), 291–296. <https://doi.org/10.1034/J.1399-3054.1997.1000210.X>
- 995 Cossani, C. M., & Reynolds, M. P. (2015). Heat stress adaptation in elite lines derived from synthetic
996 hexaploid wheat. *Crop Science*, 55(6), 2719–2735.
997 <https://doi.org/10.2135/cropsci2015.02.0092>
- 998 Cotton, T. E. A., Pétriacq, P., Cameron, D. D., Meselmani, M. al, Schwarzenbacher, R., Rolfe, S. A., &
999 Ton, J. (2019). Metabolic regulation of the maize rhizobiome by benzoxazinoids. *ISME Journal*,
1000 13(7), 1647–1658. <https://doi.org/10.1038/s41396-019-0375-2>
- 1001 Das, K., & Roychoudhury, A. (2014). Reactive oxygen species (ROS) and response of antioxidants as
1002 ROS-scavengers during environmental stress in plants. *Frontiers in Environmental Science*,
1003 2(DEC), 53. <https://doi.org/10.3389/FENVS.2014.00053/BIBTEX>
- 1004 Degen, G. E., Worrall, D., & Carmo-Silva, E. (2020a). An isoleucine residue acts as a thermal and
1005 regulatory switch in wheat Rubisco activase. *Plant Journal*, 103(2), 742–751.
1006 <https://doi.org/10.1111/tpj.14766>
- 1007 Degen, G. E., Worrall, D., & Carmo-Silva, E. (2020b). An isoleucine residue acts as a thermal and
1008 regulatory switch in wheat Rubisco activase. *Plant Journal*, 103(2), 742–751.
1009 <https://doi.org/10.1111/tpj.14766>
- 1010 Delaunay, A., Pflieger, D., Barrault, M. B., Vinh, J., & Toledano, M. B. (2002). A Thiol Peroxidase Is an
1011 H₂O₂ Receptor and Redox-Transducer in Gene Activation. *Cell*, 111(4), 471–481.
1012 [https://doi.org/10.1016/S0092-8674\(02\)01048-6](https://doi.org/10.1016/S0092-8674(02)01048-6)
- 1013 di Ferdinando, M., Brunetti, C., Fini, A., & Tattini, M. (2012). Flavonoids as Antioxidants in Plants
1014 Under Abiotic Stresses. In *Abiotic Stress Responses in Plants* (pp. 159–179). Springer New York.
1015 https://doi.org/10.1007/978-1-4614-0634-1_9
- 1016 Dogra, V., & Kim, C. (2019). Chloroplast protein homeostasis is coupled with retrograde signaling. In
1017 *Plant Signaling and Behavior* (Vol. 14, Issue 11). Taylor and Francis Inc.
1018 <https://doi.org/10.1080/15592324.2019.1656037>
- 1019 Drira, M., Saibi, W., Brini, F., Gargouri, A., Masmoudi, K., & Hanin, M. (2013). The K-segments of the
1020 wheat dehydrin DHN-5 are essential for the protection of lactate dehydrogenase and β -
1021 glucosidase activities in vitro. *Molecular Biotechnology*, 54(2), 643–650.
1022 <https://doi.org/10.1007/S12033-012-9606-8>

- 1023 Dwivedi, S., Malik, C., & Chhokar, V. (n.d.). *Molecular Structure, Biological Functions, and Metabolic*
 1024 *Regulation of Flavonoids Plant Biotechnology: Recent Advancements and Developments pp 171-*
 1025 *188 | Cite as.*
- 1026 Erena, M. F., Lohraseb, I., Munoz-Santa, I., Taylor, J. D., Emebiri, L. C., & Collins, N. C. (2021). The
 1027 WtmsDW Locus on Wheat Chromosome 2B Controls Major Natural Variation for Floret Sterility
 1028 Responses to Heat Stress at Booting Stage. *Frontiers in Plant Science, 12*.
 1029 <https://doi.org/10.3389/fpls.2021.635397>
- 1030 Eriksson, S., Eremina, N., Barth, A., Danielsson, J., & Harryson, P. (2016). Membrane-Induced Folding
 1031 of the Plant Stress Dehydrin Lti30. *Plant Physiology, 171(2)*, 932–943.
 1032 <https://doi.org/10.1104/PP.15.01531>
- 1033 Ermakova, M., Lopez-Calcagno, P. E., Raines, C. A., Furbank, R. T., & von Caemmerer, S. (2019).
 1034 Overexpression of the Rieske FeS protein of the Cytochrome b 6 f complex increases C4
 1035 photosynthesis in *Setaria viridis*. *Communications Biology, 2(1)*.
 1036 <https://doi.org/10.1038/s42003-019-0561-9>
- 1037 Eun, S. S., Choi, D., Hye, S. C., Chun, K. L., Hye, J. C., & Wang, M. H. (2007). Characterization of a
 1038 stress-responsive ankyrin repeat-containing zinc finger protein of *Capsicum annuum* (CaKR1).
 1039 *Journal of Biochemistry and Molecular Biology, 40(6)*, 952–958.
 1040 <https://doi.org/10.5483/BMBREP.2007.40.6.952>
- 1041 Geng, D., Shen, X., Xie, Y., Yang, Y., Bian, R., Gao, Y., Li, P., Sun, L., Feng, H., Ma, F., & Guan, Q. (2020).
 1042 Regulation of phenylpropanoid biosynthesis by MdMYB88 and MdMYB124 contributes to
 1043 pathogen and drought resistance in apple. *Horticulture Research, 7(1)*.
 1044 <https://doi.org/10.1038/s41438-020-0324-2>
- 1045 Gleadow, R. M., Ottman, M. J., Kimball, B. A., Wall, G. W., Pinter, P. J., Lamorte, R. L., Leavitt, S. W., &
 1046 Gleadow, R. (2015). *Drought-induced changes in nitrogen partitioning between cyanide and*
 1047 *nitrate in leaves and stems of sorghum grown at elevated CO 2 are age dependent Running*
 1048 *head: Effects of drought and CO 2 on sorghum composition.* [http://www.elsevier.com/open-](http://www.elsevier.com/open-access/userlicense/1.0/2)
 1049 [access/userlicense/1.0/2](http://www.elsevier.com/open-access/userlicense/1.0/2)
- 1050 Golan, I., Guadalupe Dominguez, P., Konrad, Z., Shkolnik-Inbar, D., Carrari, F., & Bar-Zvi, D. (2014).
 1051 Tomato ABCISIC ACID STRESS RIPENING (ASR) Gene Family Revisited. *PLoS ONE, 9(10)*,
 1052 107117. <https://doi.org/10.1371/JOURNAL.PONE.0107117>
- 1053 González-Schain, N., Dreni, L., Lawas, L. M. F., Galbiati, M., Colombo, L., Heuer, S., Jagadish, K. S. V.,
 1054 & Kater, M. M. (2016). Genome-wide transcriptome analysis during anthesis reveals new
 1055 insights into the molecular basis of heat stress responses in tolerant and sensitive rice varieties.
 1056 *Plant and Cell Physiology, 57(1)*, 57–68. <https://doi.org/10.1093/pcp/pcv174>
- 1057 Guo, R., Shi, L. X., Jiao, Y., Li, M. X., Zhong, X. L., Gu, F. X., Liu, Q., Xia, X., & Li, H. R. (2018). Metabolic
 1058 responses to drought stress in the tissues of drought-tolerant and drought-sensitive wheat
 1059 genotype seedlings. *AoB PLANTS, 10(2)*. <https://doi.org/10.1093/aobpla/ply016>
- 1060 Hara, M., Fujinaga, M., & Kuboi, T. (2004). Radical scavenging activity and oxidative modification of
 1061 citrus dehydrin. *Plant Physiology and Biochemistry, 42(7–8)*, 657–662.
 1062 <https://doi.org/10.1016/J.PLAPHY.2004.06.004>

- 1063 Hara, M., Fujinaga, M., & Kuboi, T. (2005). Metal binding by citrus dehydrin with histidine-rich
 1064 domains. *Journal of Experimental Botany*, *56*(420), 2695–2703.
 1065 <https://doi.org/10.1093/JXB/ERI262>
- 1066 Hasanuzzaman, M., Bhuyan, M. H. M. B., Zulfiqar, F., Raza, A., Mohsin, S. M., al Mahmud, J., Fujita,
 1067 M., & Fotopoulos, V. (2020). Reactive oxygen species and antioxidant defense in plants under
 1068 abiotic stress: Revisiting the crucial role of a universal defense regulator. In *Antioxidants* (Vol. 9,
 1069 Issue 8, pp. 1–52). MDPI. <https://doi.org/10.3390/antiox9080681>
- 1070 Hashimoto, Y., & Shudot, K. (1996). *CHEMISTRY OF BIOLOGICALLY ACTIVE BENZOXAZINOIDS* (Vol. 43,
 1071 Issue 3).
- 1072 Hassall, K. L., & Mead, A. (2018). Beyond the one-way ANOVA for 'omics data. *BMC Bioinformatics*,
 1073 *19*(7), 109–126. <https://doi.org/10.1186/S12859-018-2173-7/FIGURES/7>
- 1074 Hatzfeld, Y., & Saito, K. (2000). Evidence for the existence of rhodanese (thiosulfate:cyanide
 1075 sulfurtransferase) in plants: preliminary characterization of two rhodanese cDNAs from
 1076 *Arabidopsis thaliana*. *FEBS Letters*, *470*(2), 147–150. [https://doi.org/10.1016/S0014-5793\(00\)01311-9](https://doi.org/10.1016/S0014-5793(00)01311-9)
- 1078 Hinch, D. K., Gerday, C., Davies, P. L., Knight, M., Hinch, D. K., Creissen, G., Tanghe, A., & Warren,
 1079 G. (2002). Cryoprotectin: A plant lipid-transfer protein homologue that stabilizes membranes
 1080 during freezing. *Philosophical Transactions of the Royal Society B: Biological Sciences*,
 1081 *357*(1423), 909–916. <https://doi.org/10.1098/rstb.2002.1079>
- 1082 Hinch, D. K., Neukamm, B., Srór, H. A. M., Sieg, F., Weckwarth, W., Rückels, M., Lullien-Pellerin, V.,
 1083 Schröder, W., & Schmitt, J. M. (2001). Cabbage cryoprotectin is a member of the nonspecific
 1084 plant lipid transfer protein gene family. *Plant Physiology*, *125*(2), 835–846.
 1085 <https://doi.org/10.1104/pp.125.2.835>
- 1086 Hu, C., Shi, J., Quan, S., Cui, B., Kleessen, S., Nikoloski, Z., Tohge, T., Alexander, D., Guo, L., Lin, H.,
 1087 Wang, J., Cui, X., Rao, J., Luo, Q., Zhao, X., Fernie, A. R., & Zhang, D. (2014). Metabolic variation
 1088 between japonica and indica rice cultivars as revealed by non-targeted metabolomics. *Scientific*
 1089 *Reports*, *4*. <https://doi.org/10.1038/srep05067>
- 1090 Hu, S., Ding, Y., & Zhu, C. (2020a). Sensitivity and Responses of Chloroplasts to Heat Stress in Plants.
 1091 In *Frontiers in Plant Science* (Vol. 11). Frontiers Media S.A.
 1092 <https://doi.org/10.3389/fpls.2020.00375>
- 1093 Hu, S., Ding, Y., & Zhu, C. (2020b). Sensitivity and Responses of Chloroplasts to Heat Stress in Plants.
 1094 *Frontiers in Plant Science*, *11*, 375. <https://doi.org/10.3389/FPLS.2020.00375/BIBTEX>
- 1095 Huang, M. der, Chen, T. L. L., & Huang, A. H. C. (2013). Abundant Type III Lipid Transfer Proteins in
 1096 *Arabidopsis* Tapetum Are Secreted to the Locule and Become a Constituent of the Pollen Exine.
 1097 *Plant Physiology*, *163*(3), 1218. <https://doi.org/10.1104/PP.113.225706>
- 1098 Ibrahim, M. F., Hussain, F. H. S., Zanoni, G., & Vidari, G. (2017). The main constituents of *Tulipa*
 1099 *systola* Stapf. roots and flowers; their antioxidant activities. *Natural Product Research*, *31*(17),
 1100 2001–2007. <https://doi.org/10.1080/14786419.2016.1272107>
- 1101 Impa, S. M., Sunoj, V. S. J., Krassovskaya, I., Bheemanahalli, R., Obata, T., & Jagadish, S. V. K. (2019).
 1102 Carbon balance and source-sink metabolic changes in winter wheat exposed to high night-time

- 1103 temperature. *Plant Cell and Environment*, 42(4), 1233–1246.
 1104 <https://doi.org/10.1111/pce.13488>
- 1105 Impa, S. M., Vennapusa, A. R., Bheemanahalli, R., Sabela, D., Boyle, D., Walia, H., & Jagadish, S. V. K.
 1106 (2020). High night temperature induced changes in grain starch metabolism alters starch,
 1107 protein, and lipid accumulation in winter wheat. *Plant Cell and Environment*, 43(2), 431–447.
 1108 <https://doi.org/10.1111/pce.13671>
- 1109 Itam, M., Mega, R., Tadano, S., Abdelrahman, M., Matsunaga, S., Yamasaki, Y., Akashi, K., &
 1110 Tsujimoto, H. (2020). Metabolic and physiological responses to progressive drought stress in
 1111 bread wheat. *Scientific Reports*, 10(1). <https://doi.org/10.1038/s41598-020-74303-6>
- 1112 Iurlaro, A., de Caroli, M., Sabella, E., de Pascali, M., Rampino, P., de Bellis, L., Perrotta, C.,
 1113 Dalessandro, G., Piro, G., Fry, S. C., & Lenucci, M. S. (2016). Drought and heat differentially
 1114 affect XTH expression and XET activity and action in 3-day-old seedlings of durum wheat
 1115 cultivars with different stress susceptibility. *Frontiers in Plant Science*, 7(NOVEMBER2016).
 1116 <https://doi.org/10.3389/fpls.2016.01686>
- 1117 Jagadish, S. V. K., Raveendran, M., Oane, R., Wheeler, T. R., Heuer, S., Bennett, J., & Craufurd, P. Q.
 1118 (2010). Physiological and proteomic approaches to address heat tolerance during anthesis in
 1119 rice (*Oryza sativa* L.). *Journal of Experimental Botany*, 61(1), 143–156.
 1120 <https://doi.org/10.1093/jxb/erp289>
- 1121 Jain, M., Ghanashyam, C., & Bhattacharjee, A. (2010). Comprehensive expression analysis suggests
 1122 overlapping and specific roles of rice glutathione S-transferase genes during development and
 1123 stress responses. *BMC Genomics*, 11(1). <https://doi.org/10.1186/1471-2164-11-73>
- 1124 Janni, M., Gulli, M., Maestri, E., Marmioli, M., Valliyodan, B., Nguyen, H. T., Marmioli, N., & Foyer,
 1125 C. (2020). Molecular and genetic bases of heat stress responses in crop plants and breeding for
 1126 increased resilience and productivity. In *Journal of Experimental Botany* (Vol. 71, Issue 13, pp.
 1127 3780–3802). Oxford University Press. <https://doi.org/10.1093/jxb/eraa034>
- 1128 Jeevitha, D., Sadasivam, K., & Praveena, R. (2017). DFT studies on role of methoxy group in radical
 1129 scavenging ability of quebrachitol and viscumitol. In *Indian Journal of Chemistry* (Vol. 56).
- 1130 Jiang, Y., & Huang, B. (2001). Effects of calcium on antioxidant activities and water relations
 1131 associated with heat tolerance in two cool-season grasses. *Journal of Experimental Botany*,
 1132 52(355), 341–349. <https://doi.org/10.1093/JXB/52.355.341>
- 1133 Kamal, N. M., Gorafi, Y. S. A., Abdelrahman, M., Abdellatef, E., & Tsujimoto, H. (2019). Stay-green
 1134 trait: A prospective approach for yield potential, and drought and heat stress adaptation in
 1135 globally important cereals. In *International Journal of Molecular Sciences* (Vol. 20, Issue 23).
 1136 MDPI AG. <https://doi.org/10.3390/ijms20235837>
- 1137 Kaur, G., Singh, S., Singh, H., Chawla, M., Dutta, T., Kaur, H., Bender, K., Snedden, W. A., Kapoor, S.,
 1138 Pareek, A., & Singh, P. (2015). Characterization of Peptidyl-Prolyl Cis-Trans Isomerase- and
 1139 Calmodulin-Binding Activity of a Cytosolic Arabidopsis thaliana Cyclophilin AtCyp19-3. *PLOS*
 1140 *ONE*, 10(8), e0136692. <https://doi.org/10.1371/JOURNAL.PONE.0136692>
- 1141 Kenward, M. G., & Roger, J. H. (1997). Small Sample Inference for Fixed Effects from Restricted
 1142 Maximum Likelihood. *Biometrics*, 53(3), 983. <https://doi.org/10.2307/2533558>

- 1143 Kim, D., Langmead, B., & Salzberg, S. L. (2015). HISAT: A fast spliced aligner with low memory
1144 requirements. *Nature Methods*, 12(4), 357–360. <https://doi.org/10.1038/nmeth.3317>
- 1145 Kim, H. G., Kwon, S. J., Jang, Y. J., Nam, M. H., Chung, J. H., Na, Y. C., Guo, H., & Park, O. K. (2013).
1146 GDSL LIPASE1 modulates plant immunity through feedback regulation of ethylene signaling.
1147 *Plant Physiology*, 163(4), 1776–1791. <https://doi.org/10.1104/PP.113.225649>
- 1148 Kopustinskiene, D. M., Jakstas, V., Savickas, A., & Bernatoniene, J. (2020). Flavonoids as anticancer
1149 agents. In *Nutrients* (Vol. 12, Issue 2). MDPI AG. <https://doi.org/10.3390/nu12020457>
- 1150 Kotchoni, S. O., Kuhns, C., Ditzer, A., Kirch, H. H., & Bartels, D. (2006). Over-expression of different
1151 aldehyde dehydrogenase genes in Arabidopsis thaliana confers tolerance to abiotic stress and
1152 protects plants against lipid peroxidation and oxidative stress. *Plant, Cell & Environment*, 29(6),
1153 1033–1048. <https://doi.org/10.1111/J.1365-3040.2005.01458.X>
- 1154 Kumar, A., Sharma, S., Chunduri, V., Kaur, A., Kaur, S., Malhotra, N., Kumar, A., Kapoor, P., Kumari,
1155 A., Kaur, J., Sonah, H., & Garg, M. (2020a). Genome-wide Identification and Characterization of
1156 Heat Shock Protein Family Reveals Role in Development and Stress Conditions in Triticum
1157 aestivum L. *Scientific Reports 2020 10:1*, 10(1), 1–12. <https://doi.org/10.1038/s41598-020-64746-2>
- 1158
- 1159 Kumar, A., Sharma, S., Chunduri, V., Kaur, A., Kaur, S., Malhotra, N., Kumar, A., Kapoor, P., Kumari,
1160 A., Kaur, J., Sonah, H., & Garg, M. (2020b). Genome-wide Identification and Characterization of
1161 Heat Shock Protein Family Reveals Role in Development and Stress Conditions in Triticum
1162 aestivum L. *Scientific Reports*, 10(1). <https://doi.org/10.1038/s41598-020-64746-2>
- 1163 Kumar, N., & Pruthi, V. (2014). Potential applications of ferulic acid from natural sources. In
1164 *Biotechnology Reports* (Vol. 4, Issue 1, pp. 86–93). Elsevier B.V.
1165 <https://doi.org/10.1016/j.btre.2014.09.002>
- 1166 Kurek, I., Aviezer, K., Erel, N., Herman, E., & Breiman, A. (1999). The Wheat Peptidyl Prolyl cis-trans-
1167 Isomerase FKBP77 Is Heat Induced and Developmentally Regulated. *Plant Physiology*, 119(2),
1168 693. <https://doi.org/10.1104/PP.119.2.693>
- 1169 Larsen, E., & Christensen, L. P. (2000). Simple method for large scale isolation of the cyclic
1170 arylhydroxamic acid DIMBOA from maize (*Zea mays* L.). *Journal of Agricultural and Food*
1171 *Chemistry*, 48(6), 2556–2558. <https://doi.org/10.1021/jf0000934>
- 1172 Law, R. D., & Crafts-Brandner, S. J. (1999). Inhibition and Acclimation of Photosynthesis to Heat
1173 Stress Is Closely Correlated with Activation of Ribulose-1,5-Bisphosphate
1174 Carboxylase/Oxygenase. *Plant Physiology*, 120(1), 173–182.
1175 <https://doi.org/10.1104/PP.120.1.173>
- 1176 le Roy, J., Huss, B., Creach, A., Hawkins, S., & Neutelings, G. (2016). Glycosylation is a major regulator
1177 of phenylpropanoid availability and biological activity in plants. In *Frontiers in Plant Science*
1178 (Vol. 7, Issue MAY2016). Frontiers Research Foundation.
1179 <https://doi.org/10.3389/fpls.2016.00735>
- 1180 Lee, S. Y., Hwang, I. Y., & Jeong, C. S. (2017). Protective effects of cinnamic acid derivatives on gastric
1181 lesion. *Natural Product Sciences*, 23(4), 299–305. <https://doi.org/10.20307/nps.2017.23.4.299>
- 1182 Li, B., Fan, R., Sun, G., Sun, T., Fan, Y., Bai, S., Guo, S., Huang, S., Liu, J., Zhang, H., Wang, P., Zhu, X., &
1183 Song, C. peng. (2021). Flavonoids improve drought tolerance of maize seedlings by regulating

- 1184 the homeostasis of reactive oxygen species. *Plant and Soil*, 461(1–2), 389–405.
 1185 <https://doi.org/10.1007/s11104-020-04814-8>
- 1186 Liu, J. X., & Howell, S. H. (2010). Endoplasmic reticulum protein quality control and its relationship to
 1187 environmental stress responses in plants. *Plant Cell*, 22(9), 2930–2942.
 1188 <https://doi.org/10.1105/tpc.110.078154>
- 1189 Ma, D., Sun, D., Wang, C., Li, Y., & Guo, T. (2014). Expression of flavonoid biosynthesis genes and
 1190 accumulation of flavonoid in wheat leaves in response to drought stress. *Plant Physiology and*
 1191 *Biochemistry*, 80, 60–66. <https://doi.org/10.1016/j.plaphy.2014.03.024>
- 1192 Ma, R., Yuan, H., An, J., Hao, X., & Li, H. (2018). A *Gossypium hirsutum* GDSL lipase/hydrolase gene
 1193 (GhGLIP) appears to be involved in promoting seed growth in *Arabidopsis*. *PLoS ONE*, 13(4).
 1194 <https://doi.org/10.1371/JOURNAL.PONE.0195556>
- 1195 Ma, X., Xia, H., Liu, Y., Wei, H., Zheng, X., Song, C., Chen, L., Liu, H., & Luo, L. (2016). Transcriptomic
 1196 and metabolomic studies disclose key metabolism pathways contributing to well-maintained
 1197 photosynthesis under the drought and the consequent drought-tolerance in rice. *Frontiers in*
 1198 *Plant Science*, 7(DECEMBER2016). <https://doi.org/10.3389/fpls.2016.01886>
- 1199 Makowska, B., Bakera, B., & Rakoczy-Trojanowska, M. (2015). The genetic background of
 1200 benzoxazinoid biosynthesis in cereals. In *Acta Physiologiae Plantarum* (Vol. 37, Issue 9). Polish
 1201 Academy of Sciences, Institute of Slavic Studies. <https://doi.org/10.1007/s11738-015-1927-3>
- 1202 Martinez, V., Mestre, T. C., Rubio, F., Girones-Vilaplana, A., Moreno, D. A., Mittler, R., & Rivero, R. M.
 1203 (2016). Accumulation of flavonols over hydroxycinnamic acids favors oxidative damage
 1204 protection under abiotic stress. *Frontiers in Plant Science*, 7(JUNE2016).
 1205 <https://doi.org/10.3389/fpls.2016.00838>
- 1206 Masson-Delmotte, V., Zhai, P., Pörtner, H.-O., Roberts, D., Skea, J., Shukla, P. R., Pirani, A.,
 1207 Moufouma-Okia, W., Péan, C., Pidcock, R., Connors, S., Matthews, J. B. R., Chen, Y., Zhou, X.,
 1208 Gomis, M. I., Lonnoy, E., Maycock, T., Tignor, M., & Waterfield, T. (2019). *Global warming of*
 1209 *1.5°C An IPCC Special Report on the impacts of global warming of 1.5°C above pre-industrial*
 1210 *levels and related global greenhouse gas emission pathways, in the context of strengthening*
 1211 *the global response to the threat of climate change, sustainable development, and efforts to*
 1212 *eradicate poverty Edited by Science Officer Science Assistant Graphics Officer Working Group I*
 1213 *Technical Support Unit.* www.environmentalgraphiti.org
- 1214 Meiri, D., & Breiman, A. (2009). *Arabidopsis* ROF1 (FKBP62) modulates thermotolerance by
 1215 interacting with HSP90.1 and affecting the accumulation of HsfA2-regulated sHSPs. *Plant*
 1216 *Journal*, 59(3), 387–399. <https://doi.org/10.1111/j.1365-313X.2009.03878.x>
- 1217 Moore, C. E., Meacham-Hensold, K., Lemonnier, P., Slattery, R. A., Benjamin, C., Bernacchi, C. J.,
 1218 Lawson, T., & Cavanagh, A. P. (2021). The effect of increasing temperature on crop
 1219 photosynthesis: from enzymes to ecosystems. *Journal of Experimental Botany*, 72(8), 2822–
 1220 2844. <https://doi.org/10.1093/JXB/ERAB090>
- 1221 Morrell, R., & Sadanandom, A. (2019). Dealing With Stress: A Review of Plant SUMO Proteases.
 1222 *Frontiers in Plant Science*, 10. <https://doi.org/10.3389/FPLS.2019.01122>
- 1223 Nakabayashi, R., Yonekura-Sakakibara, K., Urano, K., Suzuki, M., Yamada, Y., Nishizawa, T., Matsuda,
 1224 F., Kojima, M., Sakakibara, H., Shinozaki, K., Michael, A. J., Tohge, T., Yamazaki, M., & Saito, K.

- 1225 (2014). Enhancement of oxidative and drought tolerance in Arabidopsis by overaccumulation of
1226 antioxidant flavonoids. *Plant Journal*, 77(3), 367–379. <https://doi.org/10.1111/tpj.12388>
- 1227 Nakajima, E., Iqbal, Z., Araya, H., Hiradate, S., Hamano, M., & Fujii, Y. (2005). Isolation and
1228 identification of a plant growth promotive substance from mixture of essential plant oils. *Plant*
1229 *Growth Regulation*, 45(1), 47–51. <https://doi.org/10.1007/s10725-004-7087-x>
- 1230 Naranjo, M. Á., Forment, J., Roldán, M., Serrano, R., & Vicente, O. (2006). Overexpression of
1231 Arabidopsis thaliana LTL1, a salt-induced gene encoding a GDSL-motif lipase, increases salt
1232 tolerance in yeast and transgenic plants. *Plant, Cell and Environment*, 29(10), 1890–1900.
1233 <https://doi.org/10.1111/J.1365-3040.2006.01565.X>
- 1234 Narayanan, S., Prasad, P. V. V., Fritz, A. K., Boyle, D. L., & Gill, B. S. (2015). Impact of high night-time
1235 and high daytime temperature stress on winter wheat. *Journal of Agronomy and Crop Science*,
1236 201(3), 206–218. <https://doi.org/10.1111/JAC.12101>
- 1237 Narayanan, S., Prasad, P. V. V., & Welti, R. (2016). Wheat leaf lipids during heat stress: II. Lipids
1238 experiencing coordinated metabolism are detected by analysis of lipid co-occurrence. *Plant Cell*
1239 *and Environment*, 39(3), 608–617. <https://doi.org/10.1111/PCE.12648>
- 1240 Narayanan, S., Prasad, P. V. V., & Welti, R. (2018). Alterations in wheat pollen lipidome during high
1241 day and night temperature stress. *Plant Cell and Environment*, 41(8), 1749–1761.
1242 <https://doi.org/10.1111/PCE.13156>
- 1243 Narayanan, S., Tamura, P. J., Roth, M. R., Prasad, P. V. V., & Welti, R. (2016). Wheat leaf lipids during
1244 heat stress: I. High day and night temperatures result in major lipid alterations. *Plant, Cell &*
1245 *Environment*, 39(4), 787–803. <https://doi.org/10.1111/PCE.12649>
- 1246 Niculaes, C., Abramov, A., Hannemann, L., & Frey, M. (2018). Plant protection by benzoxazinoids—
1247 recent insights into biosynthesis and function. In *Agronomy* (Vol. 8, Issue 8). MDPI AG.
1248 <https://doi.org/10.3390/agronomy8080143>
- 1249 Niu, Y., & Xiang, Y. (2018). An overview of biomembrane functions in plant responses to high-
1250 temperature stress. *Frontiers in Plant Science*, 9, 915.
1251 <https://doi.org/10.3389/FPLS.2018.00915/BIBTEX>
- 1252 Nutricati, E., Miceli, A., Blando, F., & de Bellis, L. (2006). Characterization of two Arabidopsis thaliana
1253 glutathione S-transferases. *Plant Cell Reports*, 25(9), 997–1005.
1254 <https://doi.org/10.1007/s00299-006-0146-1>
- 1255 Osato, Y., Yokoyama, R., Nishitani, K., & Nishitani, K. (2006). A principal role for AtXTH18 in
1256 Arabidopsis thaliana root growth: a functional analysis using RNAi plants Yasue Osato •
1257 Ryusuke Yokoyama • Kazuhiko Nishitani. *J Plant Res*, 119, 153–162.
1258 <https://doi.org/10.1007/s10265-006-0262-6>
- 1259 Oszvald, M., Hassall, K. L., Hughes, D., Torres-Ballesteros, A., Clark, I., Riche, A. B., & Heuer, S. (2022).
1260 Genetic Diversity in Nitrogen Fertiliser Responses and N Gas Emission in Modern Wheat.
1261 *Frontiers in Plant Science*, 0, 240. <https://doi.org/10.3389/FPLS.2022.816475>
- 1262 Park, S. Y., Noh, K. J., Yoo, J. H., Yu, J. W., Lee, B. W., Kim, J. G., Hak, S. S., & Paek, N. C. (2006). Rapid
1263 upregulation of Dehydrin3 and Dehydrin4 in response to dehydration is a characteristic of
1264 drought-tolerant genotypes in barley. *Journal of Plant Biology*, 49(6), 455–462.
1265 <https://doi.org/10.1007/BF03031126>

- 1266 Perdomo, J. A., Capó-Bauçà, S., Carmo-Silva, E., & Galmés, J. (2017). Rubisco and rubisco activase
1267 play an important role in the biochemical limitations of photosynthesis in rice, wheat, and
1268 maize under high temperature and water deficit. *Frontiers in Plant Science*, *8*.
1269 <https://doi.org/10.3389/fpls.2017.00490>
- 1270 Pobre, K. F. R., Poet, G. J., & Hendershot, L. M. (2019). The endoplasmic reticulum (ER) chaperone
1271 BiP is a master regulator of ER functions: Getting by with a little help from ERdj friends. *The*
1272 *Journal of Biological Chemistry*, *294*(6), 2098. <https://doi.org/10.1074/JBC.REV118.002804>
- 1273 Prasad, P. V. V., Pisipati, S. R., Ristic, Z., Bukovnik, U., & Fritz, A. K. (2008). Impact of nighttime
1274 temperature on physiology and growth of spring wheat. *Crop Science*, *48*(6), 2372–2380.
1275 <https://doi.org/10.2135/cropsci2007.12.0717>
- 1276 Qaseem, M. F., Qureshi, R., & Shaheen, H. (2019). Effects of Pre-Anthesis Drought, Heat and Their
1277 Combination on the Growth, Yield and Physiology of diverse Wheat (*Triticum aestivum* L.)
1278 Genotypes Varying in Sensitivity to Heat and drought stress. *Scientific Reports*, *9*(1).
1279 <https://doi.org/10.1038/s41598-019-43477-z>
- 1280 Qin, Y. xiang, & Qin, F. (2016). Dehydrins from wheat x *Thinopyrum ponticum* amphiploid increase
1281 salinity and drought tolerance under their own inducible promoters without growth
1282 retardation. *Plant Physiology and Biochemistry*, *99*, 142–149.
1283 <https://doi.org/10.1016/J.PLAPHY.2015.12.011>
- 1284 Qu, Y., Sakoda, K., Fukayama, H., Kondo, E., Suzuki, Y., Makino, A., Terashima, I., & Yamori, W.
1285 (2021). Overexpression of both Rubisco and Rubisco activase rescues rice photosynthesis and
1286 biomass under heat stress. *Plant Cell and Environment*, *44*(7), 2308–2320.
1287 <https://doi.org/10.1111/pce.14051>
- 1288 Rao, M. J., Xu, Y., Tang, X., Huang, Y., Liu, J., Deng, X., & Xu, Q. (2020). CSCYT75B1, a citrus
1289 CYTOCHROME P450 gene, is involved in accumulation of antioxidant flavonoids and induces
1290 drought tolerance in transgenic arabidopsis. *Antioxidants*, *9*(2).
1291 <https://doi.org/10.3390/antiox9020161>
- 1292 Read, A., & Schröder, M. (2021). *biology The Unfolded Protein Response: An Overview*.
1293 <https://doi.org/10.3390/biology10050384>
- 1294 Ristic, Z., Momilović, I., Bukovnik, U., Prasad, P. V. V., Fu, J., Deridder, B. P., Elthon, T. E., &
1295 Mladenov, N. (2009). Rubisco activase and wheat productivity under heat-stress conditions.
1296 *Journal of Experimental Botany*, *60*(14), 4003–4014. <https://doi.org/10.1093/jxb/erp241>
- 1297 Rohart, F., Gautier, B., Singh, A., & Lê Cao, K. A. (2017). mixOmics: An R package for ‘omics feature
1298 selection and multiple data integration. *PLoS Computational Biology*, *13*(11).
1299 <https://doi.org/10.1371/journal.pcbi.1005752>
- 1300 Rosati, V. C., Blomstedt, C. K., Møller, B. L., Garnett, T., & Gleadow, R. (2019). The Interplay Between
1301 Water Limitation, Dhurrin, and Nitrate in the Low-Cyanogenic Sorghum Mutant adult cyanide
1302 deficient class 1. *Frontiers in Plant Science*, *10*. <https://doi.org/10.3389/fpls.2019.01458>
- 1303 Routaboul, J. M., Dubos, C., Beck, G., Marquis, C., Bidzinski, P., Loudet, O., & Lepiniec, L. (2012).
1304 Metabolite profiling and quantitative genetics of natural variation for flavonoids in Arabidopsis.
1305 *Journal of Experimental Botany*, *63*(10), 3749–3764. <https://doi.org/10.1093/JXB/ERS067>

- 1306 Ruwizhi, N., & Aderibigbe, B. A. (2020). Cinnamic acid derivatives and their biological efficacy. In
 1307 *International Journal of Molecular Sciences* (Vol. 21, Issue 16, pp. 1–36). MDPI AG.
 1308 <https://doi.org/10.3390/ijms21165712>
- 1309 Sah, S. K., Reddy, K. R., & Li, J. (2016). Abscisic acid and abiotic stress tolerance in crop plants.
 1310 *Frontiers in Plant Science*, 7(MAY2016). <https://doi.org/10.3389/FPLS.2016.00571>
- 1311 Salvucci, M. E., & Crafts-Brandner, S. J. (2004a). Inhibition of photosynthesis by heat stress: the
 1312 activation state of Rubisco as a limiting factor in photosynthesis. *Physiologia Plantarum*, 120(2),
 1313 179–186. <https://doi.org/10.1111/J.0031-9317.2004.0173.X>
- 1314 Salvucci, M. E., & Crafts-Brandner, S. J. (2004b). Mechanism for deactivation of Rubisco under
 1315 moderate heat stress. *Physiologia Plantarum*, 122(4), 513–519.
 1316 <https://doi.org/10.1111/J.1399-3054.2004.00419.X>
- 1317 Sappl, P. G., Carroll, A. J., Clifton, R., Lister, R., Whelan, J., Harvey Millar, A., & Singh, K. B. (2009). The
 1318 Arabidopsis glutathione transferase gene family displays complex stress regulation and co-
 1319 silencing multiple genes results in altered metabolic sensitivity to oxidative stress. *The Plant*
 1320 *Journal*, 58(1), 53–68. <https://doi.org/10.1111/j.1365-313x.2008.03761.x>
- 1321 Scafaro, A. P., Bautsoens, N., Boer, B. den, van Rie, J., & Gallé, A. (2019). A conserved sequence from
 1322 heat-adapted species improves Rubisco activase thermostability in wheat. *Plant Physiology*,
 1323 181(1), 43–54. <https://doi.org/10.1104/pp.19.00425>
- 1324 Seong, E. S., Cho, H. S., Choi, D., Joung, Y. H., Lim, C. K., Hur, J. H., & Wang, M. H. (2007). Tomato
 1325 plants overexpressing CaKR1 enhanced tolerance to salt and oxidative stress. *Biochemical and*
 1326 *Biophysical Research Communications*, 363(4), 983–988.
 1327 <https://doi.org/10.1016/J.BBRC.2007.09.104>
- 1328 Shahidi, F. ; , Costa De Camargo, A. ; , Fuentes, J., Speisky, H., Shahidi, F., Costa De Camargo, A., &
 1329 Fuentes, J. (2022). Citation: Speisky, H Revisiting the Oxidation of Flavonoids: Loss, Conservation
 1330 or Enhancement of Their Antioxidant Properties. <https://doi.org/10.3390/antiox>
- 1331 Sharkey, T. D. (2005). Effects of moderate heat stress on photosynthesis: Importance of thylakoid
 1332 reactions, rubisco deactivation, reactive oxygen species, and thermotolerance provided by
 1333 isoprene. *Plant, Cell and Environment*, 28(3), 269–277. <https://doi.org/10.1111/J.1365-3040.2005.01324.X>
- 1335 Sharma, A., Shahzad, B., Rehman, A., Bhardwaj, R., Landi, M., & Zheng, B. (2019). Response of
 1336 phenylpropanoid pathway and the role of polyphenols in plants under abiotic stress. In
 1337 *Molecules* (Vol. 24, Issue 13). MDPI AG. <https://doi.org/10.3390/molecules24132452>
- 1338 Sharma, R., Sahoo, A., Devendran, R., & Jain, M. (2014). Over-expression of a rice tau class
 1339 glutathione s-transferase gene improves tolerance to salinity and oxidative stresses in
 1340 Arabidopsis. *PLoS One*, 9(3), e92900. <https://doi.org/10.1371/journal.pone.0092900>
- 1341 Shirdelmoghanloo, H., Cozzolino, D., Lohraseb, I., & Collins, N. C. (2016). Truncation of grain filling in
 1342 wheat (*Triticum aestivum*) triggered by brief heat stress during early grain filling: Association
 1343 with senescence responses and reductions in stem reserves. *Functional Plant Biology*, 43(10),
 1344 919–930. <https://doi.org/10.1071/FP15384>
- 1345 Skopelitou, K., Muleta, A. W., Papageorgiou, A. C., Chronopoulou, E. G., Pavli, O., Flietakis, E.,
 1346 Skaracis, G. N., & Labrou, N. E. (2017). Characterization and functional analysis of a

- 1347 recombinant tau class glutathione transferase GmGSTU2-2 from Glycine max. *International*
 1348 *Journal of Biological Macromolecules*, 94, 802–812.
 1349 <https://doi.org/10.1016/j.ijbiomac.2016.04.044>
- 1350 Sohail, M. N., Quinn, A. A., Blomstedt, C. K., & Gleadow, R. M. (2022). Dhurrin increases but does not
 1351 mitigate oxidative stress in droughted Sorghum bicolor. *Planta*, 255(4).
 1352 <https://doi.org/10.1007/s00425-022-03844-z>
- 1353 Solomon, M., Belenghi, B., Delledonne, M., Menachem, E., & Levine, A. (1999). The involvement of
 1354 cysteine proteases and protease inhibitor genes in the regulation of programmed cell death in
 1355 plants. *The Plant Cell*, 11(3), 431. <https://doi.org/10.1105/TPC.11.3.431>
- 1356 Srinivasulu, C., Ramgopal, M., Ramanjaneyulu, G., Anuradha, C. M., & Suresh Kumar, C. (2018).
 1357 Syringic acid (SA) – A Review of Its Occurrence, Biosynthesis, Pharmacological and Industrial
 1358 Importance. In *Biomedicine and Pharmacotherapy* (Vol. 108, pp. 547–557). Elsevier Masson
 1359 SAS. <https://doi.org/10.1016/j.biopha.2018.09.069>
- 1360 Sror, H. A. M., Tischendorf, G., Sieg, F., Schmitt, J. M., & Hinch, D. K. (2003). Cryoprotectin protects
 1361 thylakoids during a freeze-thaw cycle by a mechanism involving stable membrane binding.
 1362 *Cryobiology*, 47(3), 191–203. <https://doi.org/10.1016/J.CRYOBIO.2003.09.005>
- 1363 Sun, A. Z., & Guo, F. Q. (2016). Chloroplast retrograde regulation of heat stress responses in plants.
 1364 In *Frontiers in Plant Science* (Vol. 7, Issue MAR2016). Frontiers Media S.A.
 1365 <https://doi.org/10.3389/fpls.2016.00398>
- 1366 Sunkar, R., Bartels, D., & Kirch, H. H. (2003). Overexpression of a stress-inducible aldehyde
 1367 dehydrogenase gene from Arabidopsis thaliana in transgenic plants improves stress tolerance.
 1368 *Plant Journal*, 35(4), 452–464. <https://doi.org/10.1046/j.1365-3113.2003.01819.x>
- 1369 Takahashi, T., & Kakehi, J. I. (2010). Polyamines: Ubiquitous polycations with unique roles in growth
 1370 and stress responses. In *Annals of Botany* (Vol. 105, Issue 1, pp. 1–6).
 1371 <https://doi.org/10.1093/aob/mcp259>
- 1372 Teponno, R. B., Kusari, S., & Spiteller, M. (2016). Recent advances in research on lignans and
 1373 neolignans. In *Natural Product Reports* (Vol. 33, Issue 9, pp. 1044–1092). Royal Society of
 1374 Chemistry. <https://doi.org/10.1039/c6np00021e>
- 1375 Theis, J., & Schroda, M. (2016). Revisiting the photosystem II repair cycle. In *Plant Signaling and*
 1376 *Behavior* (Vol. 11, Issue 9). Taylor and Francis Inc.
 1377 <https://doi.org/10.1080/15592324.2016.1218587>
- 1378 Tschaplinski, T. J., Abraham, P. E., Jawdy, S. S., Gunter, L. E., Martin, M. Z., Engle, N. L., Yang, X., &
 1379 Tuskan, G. A. (2019). The nature of the progression of drought stress drives differential
 1380 metabolomic responses in Populus deltoides. *Annals of Botany*, 124(4), 617–626.
 1381 <https://doi.org/10.1093/aob/mcz002>
- 1382 Valente, M. A. S., Faria, J. A. Q. A., Soares-Ramos, J. R. L., Reis, P. A. B., Pinheiro, G. L., Piovesan, N.
 1383 D., Morais, A. T., Menezes, C. C., Cano, M. A. O., Fietto, L. G., Loureiro, M. E., Aragão, F. J. L., &
 1384 Fontes, E. P. B. (2009). The ER luminal binding protein (BiP) mediates an increase in drought
 1385 tolerance in soybean and delays drought-induced leaf senescence in soybean and tobacco.
 1386 *Journal of Experimental Botany*, 60(2), 533. <https://doi.org/10.1093/JXB/ERN296>

- 1387 van den Ende, W. (2013). Multifunctional fructans and raffinose family oligosaccharides. *Frontiers in*
1388 *Plant Science*, 4(JUL). <https://doi.org/10.3389/FPLS.2013.00247>
- 1389 van Sandt, V. S. T., Suslov, D., Verbelen, J. P., & Vissenberg, K. (2007). Xyloglucan
1390 Endotransglucosylase Activity Loosens a Plant Cell Wall. *Annals of Botany*, 100(7), 1467.
1391 <https://doi.org/10.1093/AOB/MCM248>
- 1392 Vissenberg, K., Fry, S. C., Pauly, M., Höfte, H., & Verbelen, J. P. (2005). XTH acts at the microfibril-
1393 matrix interface during cell elongation. *Journal of Experimental Botany*, 56(412), 673–683.
1394 <https://doi.org/10.1093/JXB/ERI048>
- 1395 Vissenberg, K., Oyama, M., Osato, Y., Yokoyama, R., Verbelen, J. P., & Nishitani, K. (2005). Differential
1396 expression of AtXTH17, AtXTH18, AtXTH19 and AtXTH20 genes in Arabidopsis roots.
1397 Physiological roles in specification in cell wall construction. *Plant & Cell Physiology*, 46(1), 192–
1398 200. <https://doi.org/10.1093/PCP/PCI013>
- 1399 Wan, X., Wu, S., Li, Z., An, X., & Tian, Y. (2020). Lipid Metabolism: Critical Roles in Male Fertility and
1400 Other Aspects of Reproductive Development in Plants. *Molecular Plant*, 13(7), 955–983.
1401 <https://doi.org/10.1016/J.MOLP.2020.05.009>
- 1402 Wang, J., Yuan, B., & Huang, B. (2019). Differential heat-induced changes in phenolic acids associated
1403 with genotypic variations in heat tolerance for hard fescue. *Crop Science*, 59(2), 667–674.
1404 <https://doi.org/10.2135/cropsci2018.01.0063>
- 1405 Wang, X., & Liu, F. (2021). Effects of elevated co2 and heat on wheat grain quality. In *Plants* (Vol. 10,
1406 Issue 5). MDPI AG. <https://doi.org/10.3390/plants10051027>
- 1407 Wang, X., Xu, C., Cai, X., Wang, Q., & Dai, S. (2017). Heat-responsive photosynthetic and signaling
1408 pathways in plants: Insight from proteomics. In *International Journal of Molecular Sciences*
1409 (Vol. 18, Issue 10). MDPI AG. <https://doi.org/10.3390/ijms18102191>
- 1410 Waters, E. R., & Vierling, E. (2020). Plant small heat shock proteins – evolutionary and functional
1411 diversity. *New Phytologist*, 227(1), 24–37. <https://doi.org/10.1111/NPH.16536>
- 1412 Watkins, J. L., Li, M., McQuinn, R. P., Chan, K. X., McFarlane, H. E., Ermakova, M., Furbank, R. T.,
1413 Mares, D., Dong, C., Chalmers, K. J., Sharp, P., Mather, D. E., & Pogson, B. J. (2019). A GDSL
1414 esterase/lipase catalyzes the esterification of lutein in bread wheat. *Plant Cell*, 31(12), 3092–
1415 3112. <https://doi.org/10.1105/TPC.19.00272>
- 1416 Xu, J., Henry, A., & Sreenivasulu, N. (2020). Rice yield formation under high day and night
1417 temperatures—A prerequisite to ensure future food security. In *Plant Cell and Environment*
1418 (Vol. 43, Issue 7, pp. 1595–1608). Blackwell Publishing Ltd. <https://doi.org/10.1111/pce.13748>
- 1419 Xu, J., Misra, G., Sreenivasulu, N., & Henry, A. (2021). What happens at night? Physiological
1420 mechanisms related to maintaining grain yield under high night temperature in rice. *Plant Cell*
1421 *and Environment*, 44(7), 2245–2261. <https://doi.org/10.1111/pce.14046>
- 1422 Yacoubi, I., Gadaleta, A., Mathlouthi, N., Hamdi, K., & Giancaspro, A. (2022). Abscisic Acid-Stress-
1423 Ripening Genes Involved in Plant Response to High Salinity and Water Deficit in Durum and
1424 Common Wheat. *Frontiers in Plant Science*, 0, 175. <https://doi.org/10.3389/FPLS.2022.789701>
- 1425 Yan, H., Wang, C., Liu, K., & Tian, X. (2021). Detrimental effects of heat stress on grain weight and
1426 quality in rice (*Oryza sativa* L.) are aggravated by decreased relative humidity. *PeerJ*, 9.
1427 <https://doi.org/10.7717/peerj.11218>

- 1428 Yang, W., Zhang, L., Lv, H., Li, H., Zhang, Y., Xu, Y., & Yu, J. (2015). The K-segments of wheat dehydrin
1429 WZY2 are essential for its protective functions under temperature stress. *Frontiers in Plant*
1430 *Science*, 6(June). <https://doi.org/10.3389/FPLS.2015.00406/FULL>
- 1431 Yang, X., Sun, C., Hu, Y., & Lin, Z. (2008). Molecular cloning and characterization of a gene encoding
1432 RING zinc finger ankyrin protein from drought-tolerant *Artemisia desertorum*. *Journal of*
1433 *Biosciences*, 33(1), 103–112. <https://doi.org/10.1007/S12038-008-0026-7>
- 1434 Yu, Z., Wang, X., & Zhang, L. (2018). Structural and Functional Dynamics of Dehydrins: A Plant
1435 Protector Protein under Abiotic Stress. *International Journal of Molecular Sciences*, 19(11).
1436 <https://doi.org/10.3390/IJMS19113420>
- 1437 Zhai, J., Qi, Q., Wang, M., Yan, J., Li, K., & Xu, H. (2022). Overexpression of tomato thioredoxin h
1438 (SlTrxh) enhances excess nitrate stress tolerance in transgenic tobacco interacting with SlPrx
1439 protein. *Plant Science*, 315. <https://doi.org/10.1016/j.plantsci.2021.111137>
- 1440 Zhao, C., Liu, B., Piao, S., Wang, X., Lobell, D. B., Huang, Y., Huang, M., Yao, Y., Bassu, S., Ciais, P.,
1441 Durand, J. L., Elliott, J., Ewert, F., Janssens, I. A., Li, T., Lin, E., Liu, Q., Martre, P., Müller, C., ...
1442 Asseng, S. (2017). Temperature increase reduces global yields of major crops in four
1443 independent estimates. *Proceedings of the National Academy of Sciences of the United States*
1444 *of America*, 114(35), 9326–9331. <https://doi.org/10.1073/pnas.1701762114>
- 1445 Zhao, J., Long, T., Wang, Y., Tong, X., Tang, J., Li, J., Wang, H., Tang, L., Li, Z., Shu, Y., Liu, X., Li, S., Liu,
1446 H., Li, J., Wu, Y., & Zhang, J. (2020). RMS2 Encoding a GDGL Lipase Mediates Lipid Homeostasis
1447 in Anthers to Determine Rice Male Fertility. *Plant Physiology*, 182(4), 2047.
1448 <https://doi.org/10.1104/PP.19.01487>
- 1449 Zhou, S., Richter, A., & Jander, G. (2018). Beyond defense: Multiple functions of benzoxazinoids in
1450 maize metabolism. In *Plant and Cell Physiology* (Vol. 59, Issue 8, pp. 1528–1533). Oxford
1451 University Press. <https://doi.org/10.1093/pcp/pcy064>
- 1452